FLUID-STRUCTURE INTERACTION IN PERIODIC STRUCTURE

Rong Xin Lee

Bachelor of Engineering
Mechatronic Engineering

Department of Engineering
Macquarie University

November 7, 2016

Supervisor: Dr. David Inglis

ACKNOWLEDGMENTS

I would like to express my sincere gratitude to my supervisor Dr. David Inglis, for his constant guidance and encouragement throughout my undergraduate thesis project. I would also like to express my gratitude to PhD candidate, Shilun Feng and my fellow classmates, James White and Taylor Corbett for giving their best to help me in the working of the thesis project. I also like to take this opportunity to thank my parents for their unceasing encouragement and support.

STATEMENT OF CANDIDATE

I, Rong Xin Lee, declare that this report, submitted as part of the requirement for the award of Bachelor of Engineering in the Department of Engineering, Macquarie University, is entirely my own work unless otherwise referenced or acknowledged. This document has not been submitted for qualification or assessment an any academic institution.

Student's Name: Rong Xin Lee

Student's Signature: Rong Xin Lee

Date: August 26, 2016

ABSTRACT

Fluid-Structure Interaction (FSI) is defined as a combination of law of fluid dynamics and the relevant structural mechanics and the term of FSI has given the best description for itself which is the interactions between fluid and structures. Periodic structures such as Deterministic Lateral Displacement (DLD) array that is a microfluidics technology that first introduced by Huang et al. and the array enables micro-scaled particles to be sorted passively. The DLD array is fabricated in microfludics device through a series of microfabrication procedures. Here, we examine the interactions of fluorescent dyed particles in micro-sized along with the fluid flow against the DLD array, and we also examine the influence of the fluid flow behaviours on the particle movements in the arrays through fluorescence microscopy.

Micro particle tracking velocimetry (μPTV) is a measurement technique for particle velocity in micro sized. It is usually used to quantify particle to particle differences through a set of algorithms such as particle image tracking and particle image analysis. Hence, Matlab codes that based on the concept of μPTV technique are provided to run a numbers of videos which has recorded micro sized particle movement to generate the velocity vector field in DLD array The results of the vector fields that processed by Matlab codes are generally ideal, but the vectors in some areas of the image are not detected or quantified. Somehow, we haven't achieve the objective of this project which is tracking a moving particle but we are getting there. Therefore, the properties of microscopy and the algorithms in Matlab code need to be optimized for the future works.

Contents

List of Figures

List of Tables

Chapter 1

Introduction

1.1 Fluid-Structure Interaction

Fluid-Structure Interaction (FSI) is a physics phenomenon describes the interaction between a structure and internal or surrounding fluid flow. The interaction can be stable or oscillatory, this is dependent on some circumstances such as amount of the fluid, shape or size of the structure, external forces and pressure etc. In some cases, the deformation or movement on the structure can be occurred when a pressurised flowing fluid encounters the structure. The deformed or moved structure changes surrounding flow fields, then changed flow fields will generate another pressure on the structure and cause deformation or movement.

Hydrodynamics mass, also known as added mass is one of the main points in the study of FSI and fluid dynamics, it was proposed by Friedrich Bessel in 1828. He discovered that surrounding fluid increased the effective mass of the system when he was studying the motion of a pendulum in a fluid. In 1843, George Gabriel Stokes gave the concept of fluid-structure interaction with his discover, that effective mass of the object increased due to the effect of surrounding fluid by the amount of hydrodynamic mass was same as the mass of fluid it displaced [30].

Hereafter, FSI is gradually applied and considered in the design of engineerings systems that subjected to hydrodynamics, aerodynamics, and aero-elasticity. For instances, air flow causes the aircraft wings on commercial airplane deforms and the deformed wings by maximise the lift or drag, reduced lift or increasing the wing area etc. change the air flow around the wings for take-off, climbing, landing and braking. The whiskers on Ferrari 458 Italia deform to change airflow over the radiators for minimise the drag and lift [35].

Figure 1.1: Illustration of air flow on the whisker of Ferrari 458

1.2 Microfluidics and Periodic Structures

Microfluidics, the science that study the behaviour of fluid in low volume on the order of microlitres to nanolitres (10^{-6} to 10^{-9} litres) or lower in micrometres size channels. On the other hand, microfluidics also known as the technology to create the devices for applications such as lab-on-a-chip devices.

The invention of integrated transistor and the inkjet print-head technology developed at International Business Machines Corporation (IBM) are the earliest applications of microfluidics technologies, which are emerged in 1960's along with the development of photolithography technology etc. In 80's the invention of Micro Electro Mechanical Systems (MEMS) and gave a significantly expansion in the development microfluidics in the last 30 years along with the fabrication of microfluidics chip made of polydimethylsiloxane (PDMS) and attaching with glass. [14] [6]. Nowadays, microfluidics devices such as microfluidics particle separation arrays, which have been widely applied in various applications such as particle and fluid researches, medical diagnostics, and pharmaceutical industry.

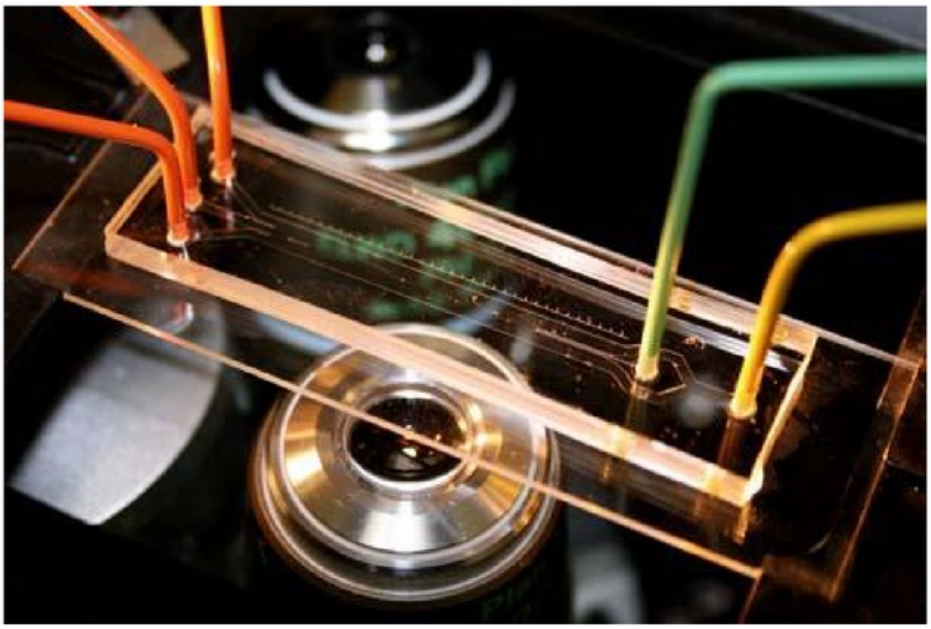

Figure 1.2: Mircofluidics devices with PDMS layer for pharmaceutical and biomedical research [4].

Periodic structures are the structures which have arranged or built in recurrence patterns and a array that set up with Deterministic Lateral Displacement (DLD) principle are periodic. The array enables micro-scaled particles to be sorted passively and displaced laterally while avoiding the pillars or posts in the arrays [28]. The flow has influence on the displacement of the particles and the flow is known as laminar flow, which is a common phenomenon of fluid flow especially occur in microfluidics due to the micro sizes, yield low Reynolds number for the flow that is used to define the flow pattern. Since the first DLD particle separation array introduced by Huang et. al, the DLD array has been extensively studied by Inglis, Davis and Beech et al. and now the array applied in various applications, for instances the separation array can be used to separate cells in blood or extract parasites or chromosomes in human body or biology experiment [22]. Besides, the Mount Sinai Ichan School of Medicine from New York teams up with IBM Research and striving for generate a lab-on-a-chip with DLD array that able separate the nano-sized particles around 20 nanometers, this project is proposed to detect the cancer markers before a tumour or even before the symptoms. [31]

1.3 Micro Particle Tracking Velocimetry

Micro particle tracking velocimetry (μPTV) is a technique for tracking particles and determine their velocity. It is usually used to quantify particle to particle differences through a set of algorithms such as particle image tracking and particle image analysis. μPTV is the derivation of particle tracking velocimetry (PTV) or known as low particle number density Particle Image Velocimetry (PIV) [12]. Both of these methods (PTV and PIV) are applied for determine the velocity from the displacement of particles in a time interval. PTV is used to track an individual particle and its trajectories in a two-dimensional plane or three-dimensional plane and PIV tracks a small group of particles.

1.4 Project Objective

In this project, the relevant theories and works of microfluidics, deterministic lateral displacement (DLD) and micro Particle Image Velocimetry (μPTV) technique are reviewed in chapter 2. The chapter followed by the description of a series of microchip fabrication procedures and the experimental setup for the experiments, see chapter 3. Besides, the chapter 4 including the vector field results and relevant discussions, then followed by the conclusion and future works suggestions for the project.

The main project objective is expected to provide a series of data of moving 0.5 microns and 7.3 microns particles activities in a DLD array microchip that simulated by μPTV technique. Hence, numbers of accompanied objectives for this project are listed as below:

- Generate velocity flow fields and corresponding vectors by using μPTV technique.
- Determine the flow field with no big particle, one accompanied by a moving big particle and one with a stationary big particle.
- Determine exception of displacement behaviour according to some publication and studies such that big particle will flow towards low flow rate lamina, if it is possible.

Chapter 2

Background and Related Work

2.1 Microfluidics Theory

2.1.1 Navier Stokes Equations

Newton's second law of motion describes the force resulting on a mass and corresponding acceleration.

$$F = ma \tag{2.1}$$

Navier Stokes equations are treated as the Newton's second law of motion for fluids. In between 1827 and 1845, Navier Stokes equations were successively derived by Navier, Poisson, Saint-Venant and Stokes [9] and the equations are also treated as the extensions of Euler equations. Since the Navier Stokes equations proposed, they are widely applied and considered in the design of engineering such as aerodynamics, hydrodynamics, and microfludics as well. The equations describe the non-relativistic motion of fluids or describe the velocity, v, and the pressure, p, in a Newtonian fluid with density, ρ and dynamic viscosity, η.

The left equation in the equation 2.2, $\rho\left[\frac{\partial v}{\partial t}+(v\cdot\nabla)v\right]$ represents the inertial acceleration consist of unsteady acceleration, $\frac{\partial v}{\partial t}$ which describes the changes of fluid velocity over time in a stationary position, yet convective acceleration, $(v \cdot \nabla)v$ represents the changes of velocity as the fluid flows from one position to another. The right hand terms in the equations are mostly represented as forces. The term of $-\nabla p$ and the term of $\eta\nabla^2$ represents the pressure gradient and viscous force respectively, summation of these two terms is presented as the divergence of stress. In addition, the term of f represents as the external forces that applied to fluid such as gravity force etc.

$$\rho\left[\frac{\partial v}{\partial t} + (v \cdot \nabla)v\right] = -\nabla p + \eta\nabla^2 + f \tag{2.2}$$

Equation 2.3 is the continuity equation that follows Navier-Stokes equations and it represents as the conservation of mass, where ρ is the fluid density and v is the velocity. The density will become constant in the fluid which is incompressible whilst continuity equation will be reduced as shown as equation 2.4.

Continuity equation:

$$\frac{\partial \rho}{\partial t} + \nabla \cdot (\rho v) = 0 \tag{2.3}$$

Continuity equation for incompressible fluid:

$$\nabla \cdot v = 0 \tag{2.4}$$

2.1.2 Flow Regimes and Reynolds Number

Motion of fluids or fluid flows can be categorised into different flow regimes, laminar flow, turbulent flow and transitional flow sometimes, these are the most general types of fluid flows. The fluid flow presents with layers of fluids that flow is parallel without disruptions or mixing between the layers, this is known as laminar flow or streamline flow. Inversely, turbulent flow has the flow with disruptions, fluctuations or unpredictable and transitional flow describes the mixing of laminar and turbulent flow. These flow regimes can be determined by Reynolds Number.

Figure 2.1: Turbulent flow around the submarine. Image from Wikipedia [42].

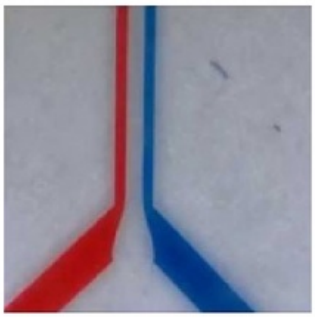

Figure 2.2: Laminar flow in microchannel. Image from Elveflow [16].

The Reynolds number is named after Osborne Reynolds and was proposed with his studies of circumstances of fluid flow in pipes [34]. Reynolds number, Re is a dimensionless number which is used to measure the ratio between the inertial forces and viscous forces as shown in the following equations, where the L and V respectively represent the characteristic linear length and average velocity of the system. When a flow occurs with small viscosities, large characteristic length, and high velocity and density, the flow will have a high Reynolds number, typically greater than 2300 in the case of a round pipe and the flow is turbulent. Inversely, the laminar flow is determined when the flow has low velocities, high viscosities, small characteristic length and these give low Reynolds number at around 10 to 100 or even lower dependent on the parameters.

Inertial force can be expressed in terms of velocity and characteristic length:

$$F_{inertial} \propto \rho v \frac{\partial v}{\partial x} \quad \Rightarrow \rho \frac{V^2}{L} \tag{2.5}$$

Similarly for the viscous force:

$$F_{viscous} \propto \eta \frac{\partial^2 v}{\partial x^2} \quad \Rightarrow \eta \frac{V}{L^2} \tag{2.6}$$

Therefore, the Reynolds number or the ratio between inertial force and viscous force as shown as below:

$$\frac{F_{inertial}}{F_{viscous}} = \frac{\rho L V}{\eta} \equiv Re \tag{2.7}$$

2.1.3 Reynolds Number and Navier Stokes Equations

For the fluid flow in microfluidics, the Reynolds number will be very low due to micro-scaled dimensions of channels, low characteristic velocities of fluid and viscosities dominates the inertial forces. When Re $\ll$ 1, the fluid flow will exhibit as Stokes flow or "creeping flow" which has no lateral convection and the no interference between lamina layers or streamlines. Thus, the inertial terms in Navier Stokes equations (equation 2.2), $(v \cdot \nabla)v$ can be neglected due to low Reynolds number and the equations transform from a nonlinear partial differential equations into a simplify linear equation, which is known as linear Stokes equation (equation 2.8). In addition, the motion in the fluid are symmetric due to low Reynolds number. The motion in the fluid will be reversed as the pressure or forces applied are reversed [5]. Laminar flows including Stokes flow provide a means by a micro-sclaed object can be transported in a relatively predictable manner through microchannel.

$$0 = -\nabla p + \eta \nabla^2 \tag{2.8}$$

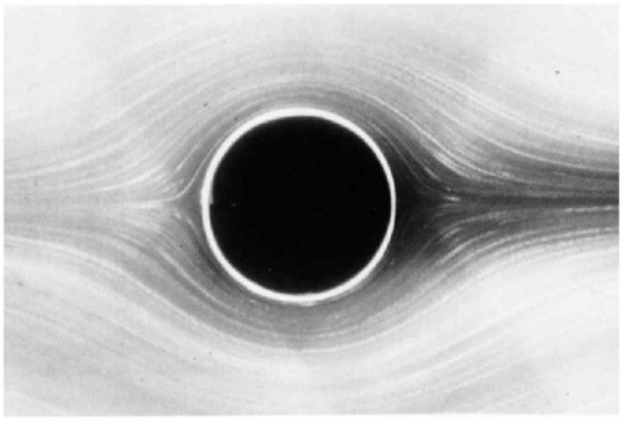

Figure 2.3: Stokes flow occurred around circular cylinder at Re = 0.16 [13]

2.1.4 Stokes' Law

Stokes's law is an expression derived by Stokes and named after him. The Stokes' law is used to measure the force acting on a spherical object that move in a viscous fluid which has given a very low Reynolds number experience a frictional force, and this force are known as viscous drag force. It is occurred in the opposite direction to the object movement, In the equation 2.9, the terms of r and v represents as the radius and velocity of spherical object respectively. Despite of dependence of the drag force on velocity of the spherical object, drag force is also dependent when additional force is applied on the object such as gravity force etc. This causes the acceleration of spherical object and the object will be forced to flow across the streamlines or lamina layers when it interacts an obstacle in microfluidics device, but then the particle will be stabilised by the drag force.

$$F_{drag} = -6\pi\eta r v \tag{2.9}$$

2.1.5 Diffusion

Since the laminar flow has low Reynolds Number, there will be little mixing between the streamlines in the flow that caused by diffusion. The time to mix by diffusion will be measured as shown as equation 2.10 to quantify the mixing by diffusion at micro-scaled, where l is the characteristic length and the diffusion coefficient, D for spherical particle which is given by the Stokes-Einstein relation, see equation 2.11.

$$Diffusion\ time = \frac{L^2}{D} \tag{2.10}$$

Diffusion coefficient:

$$D = \frac{k_B T}{6\pi\eta a} \tag{2.11}$$

The terms of k_BT in the numerator of diffusion coefficient (equation 2.11), which k_B represents the Boltzmann constant and T is the absolute temperature. The term of a represents the linear size (eg. particle radius). The Pélet number, Pe has to be high enough or else the streams or streamlines will become unclear due to diffusion. It shows the relationship between convection and diffusion time with the characteristic length, L and velocity, V and diffusion coefficient, see equation 2.12.

$$\frac{Diffusion\ time}{Convection\ time} = \frac{\frac{L^2}{D}}{\frac{L}{V}} = \frac{LV}{D} \equiv Pe \tag{2.12}$$

2.1.6 Fluidic resistance

The resistance of the fluid flow is important for designing a microfludics device or micro-sized particle separation array such as DLD array. The resistance of the fluid flow in microchannel increases when the dimensions of the channel decrease, this is because of the friction increment between the channel walls and the fluid body. The channel geometry becomes more complex and the increment of the surface area to volume ratio [32]. Thus, the resistance of the fluid flow, R can be calculated by the ratio of pressure difference, ΔP to the flow rate, Q.

$$R = \frac{\Delta P}{Q} \tag{2.13}$$

For the rectangular microchannels, the dimensions (width, w, height, h and length, l) of channels will be taken into account and the resistance can be derived as:

$$R = \frac{12\eta l}{wh^3} \tag{2.14}$$

2.2 Deterministic Lateral Displacement

Deterministic lateral displacement (DLD) is a pricinple and first introduced by Lotien Richard Huang et al. in 2004. They applied the asymmetric bifurcation of laminar flow along with periodic obstacles to separate particles on the basis of size in continuous flow with a small-scale resolution [23].

The DLD arrays use the mechanism of laminar flow to operate and the flow is divided into a number of equivalent streamlines by the pillars or array posts. The separation or travel mode of spherical particle is dependent on various circumstances such as the size of particle itself, distance between the particle and pillar, distance between the pillars and the offset. The diameter (or radius) of the particle and its centre point will decide the migrations or its travel mode within the streamlines. If the radius of particle is smaller than the critical diameter size from the pillar and which centre point of the particle is in the first streamline when it meets the pillar, then it will stay and flow along with the similar lamina and travel in zigzag mode due the bifurcation of the flow. Inversely, if

the radius of the particle are larger than the critical diameter size and the centre of the particle falls in the neighbouring streamline when it meets the pillar, then it will flow in to next neighbouring streamline as it meets the pillars in next row. This separation phenomenon is called bumping mode or displacement mode.

In the following figure 2.4, it has shown that the parameters defining the pillars and streamlines in a DLD array. The vertical arrow on the top view of the figure represents fluid flow and generate three equivalent streamlines which are labelled 1, 2, and 3. The term of λ represents the distance between the centre of the pillars. Each row is shifted by a distance, $\varepsilon\lambda$, where the term of ε represents the row shift fraction. The terms of g (or G in some other research papers) represents the distance of the gap between two pillars. A flow profile, $u(x)$ is shown and the β in the profile represents the width of the first streamlines. [29].

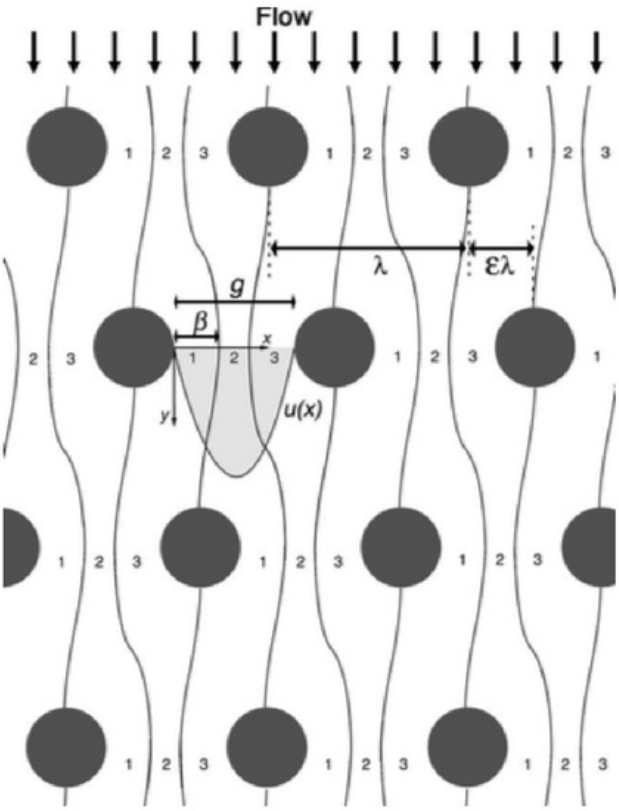

Figure 2.4: Illustration of streamlines flow through DLD array. Image from David et al.

2.2.1 Row shifted post, critical diameter size and flows in DLD array

As described in section 2.2, the post array or pillar array in the DLD is periodic. The distance between the centre of the pillars in rows and columns are equal and row are perpendicular to the fluid flow. Row shifted post is the post in the next row and shifted by a distance, $\varepsilon\lambda$, and this allows the particle with larger critical diameter size can be displaced laterally. Besides, the gap between the posts allows a numbers of streamlines flows through, which number of streamlines are dependent on the distance of the gap and this can be determined by following formula (equation 2.15), where the term of ε is represented as the row shift fraction. Thus, the row shifted fraction is usually determined by using the equation 2.16, measures an angle θ in column and this gives row fraction equal to the tangent of shifted angle:

$$N = \frac{\lambda}{\varepsilon\lambda} = \frac{1}{\varepsilon} \quad \Rightarrow \quad \varepsilon = \frac{1}{N} \tag{2.15}$$

$$\varepsilon = tan\ \theta \tag{2.16}$$

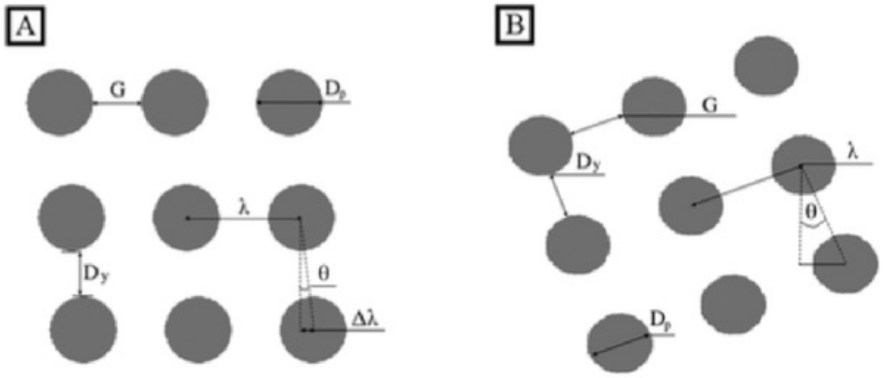

Figure 2.5: Illustration of rhombic and tilted DLD array. Image from McGrath et al.

Nonetheless, some of the DLD arrays are employing different designs such as rhombic and tilted as illustrated in figure 2.5, and the designed array sometimes gives different or smaller gap size between the pillars of column, D_y and the parameter $\Delta\lambda$ (or $\varepsilon\lambda$) does not exist in tilted array. Hence, the row shifted fraction for this case can be determined by using the equation 2.17, measures an angle θ in column with D_y divide by the λ:

$$\varepsilon = \frac{D_y tan\ \theta}{\lambda} \tag{2.17}$$

As mentioned before, critical diameter size for separation, D_c deicides the particle's travel mode (zigzag or bumping) in the DLD array. Hence, the critical diameter size can

be determined by using the width of the first streamlines, β and which is twice of the width as presented by David et al.

$$D_c = 2\beta \tag{2.18}$$

Alternatively, β can be replaced to determine the effect of the gap, g and row shift fraction, ε as the following equation and a unit less parameter α should be included to accommodate non-uniform flow through the DLD gap and correct for the corresponding flow profile.

$$D_c = 2\alpha g\varepsilon \tag{2.19}$$

As presented in figure 2.4, there are three equivalent streamline or fluid volume flux occurred between two pillars in the flow profile, $u(x)$. The total of volume flux can be defined as ϕ_{gap} and which can be divided by the total number of streamlines for finding each volume flux, ϕ_i (where i=1,2,3,... N).

$$\phi_i = \frac{1}{N}\phi_{gap} = \varepsilon\phi_{gap} \tag{2.20}$$

For instances, to obtain the width of the first streamlines, β in the flow profile, $u(x)$ as shown in the figure 2.4 by integrating the profile as equation 2.21.

$$\int_0^{\beta} u(x)dx = \varepsilon \int_0^{g} u(x)dx \tag{2.21}$$

Assuming a parabolic flow profile and zero velocity from the edge of the pillar, the width of the first streamline, β can be analytically determined, thus the flow profile can be written as:

$$u(x) = \left[\frac{g^2}{4} - \left(x - \frac{g}{2}\right)^2\right] \tag{2.22}$$

Then, solve the equation 2.21 and resulting,

$$\left[\frac{\beta}{g}\right]^3 - \frac{3}{2}\left[\frac{\beta}{g}\right]^2 + \varepsilon\frac{1}{2} = 0. \tag{2.23}$$

Apply the equation 2.18, the solution for the integral can be written as:

$$D_c = g\left[1 + 2w + \frac{1}{2w}\right], \tag{2.24}$$

where

$$w^3 = \frac{1}{8} - \frac{\varepsilon}{4} \pm \sqrt{\frac{\varepsilon}{16}(\varepsilon - 1)} \tag{2.25}$$

and the correct root of w^3 is

$$w = \left[\frac{1}{8} - \frac{\varepsilon}{4} + \sqrt{\frac{\varepsilon}{16}(\varepsilon - 1)}\right]^{\frac{1}{3}} \left(-\frac{1}{2} - i\frac{\sqrt{3}}{2}\right). \tag{2.26}$$

In the research by Davis, a numbers of DLD devices with various gap size and spherical particle size based on the parabolic profile were applied, an empirical formula was proposed by Davis for determine the critical diameter size [10], as shown:

$$D_c = 1.4g\varepsilon^{0.48} \tag{2.27}$$

2.2.2 Factors influencing the critical diameter size

Sidewall effects

The flow profile can become perturbed in the locations between the array and the sidewall, and the critical diameter size changes [28] and causes particle flow along the sidewalls beside than the displacement or zigzag mode. To reduce such effect, the DLD array side wall should be redesigned in irregular shape instead of straight wall. This helps to separate the particle effectively and also reduce the residual particles left in the DLD array. The separation from the left to right, and the width of the gap between left boundary and adjacent pillars is given by,

$$G_{left} = G\sqrt{n\varepsilon} = G\sqrt{\frac{n}{N}}. \tag{2.28}$$

The term of n represents the row number and N represents number of total streamlines. The term of G in the equation represents the nominal gap. Meanwhile, the gap width between the right boundary and adjacent pillars for right to left separation is given by,

$$G_{left} = G\sqrt{2 - n\varepsilon} = G\sqrt{2 - \frac{n}{N}}. \tag{2.29}$$

Post diameter to gap size ratio

In the research of Beech [3], shows the velocity flow profiles in various post diameter with the constant device depth and gap size and gives the result of the flow profile with larger post diameter is nearly parabolic. Another flow profile reversely becomes more plug-like when the post or pillar diameter to the gap ratio is smaller then the critical diameter size becomes reduced.

Device depth

The effect on critical diameter size that occurred by the device depth is relevant with the previous section. From the studies of Beech has shown the similar results as previous section for velocity flow profiles against the device depth and also the results fraction

of the fluid flow through the gap when post diameter and the gap size remain constant. The flow profile is more plug-like and larger fraction of the fluid flow as the device depth is decreased, thus the critical diameter size decreases. However, the device becomes too shallow to allow the particle beyond the critical diameter size to travel as the depth is decreased,

Post shape

The fluid flow velocity profile and the critical diameter size can be affected by the shape of the post. A numbers of post shapes have been applied for DLD array such as triangular post, rectangular post and most commonly circular post. Different shapes of the post results different gap size, width of the streamlines and other parameters regarding the post, and this also changes the laminar flow pattern in the array as fluid flow through. Therefore, all these effects results different critical diameter sizes.

2.2.3 Diffusion

Diffusion widens the streams of particle and leads to the migration of particles between streamlines. The particle will travel from zigzag mode to the bumping mode if the particle diffuse an absolute distance of $D_{particle} - D_c$, where $D_{particle}$ is the diameter of particle. In Beech's research, the diffusion can be ignored if the micrometre sized particles at the average flow velocities of 100 micron (μm) per second or above, resultant high Pélet number. Generally, the effects of diffusion are extremely small in a DLD array and which do not significantly affect the overall trajectory of the particles. However, the separation efficiency will reduce as the particle size decreases and diffusivity increases. To overcome that, the flow velocities can be increased.

2.2.4 Particle volume fraction

Asymmetric bifurcation are one of the elements that decides the migration of the particles in DLD arrays as mentioned in section 2.2. The particle volume fractions are not equal when spherical particle suspends at the asymmetric bifurcation with two daughter branches. However, the branches with comparable geometrical characteristics, receive different flow rates and the particles volume fraction is increase in the high flow rate branch which phenomenon is known as the Zweifach-Fung effect [11]. A numbers of calculations and experiments on a T-shaped bifurcation with different flow rates and various sizes of spherical particles were investigated and discussed by Doyeux et al. and shows that the numbers of particles are directed towards the low flow rate branch, yet majority of the particles tend to directed to hight flow rate branch. Beside, they also concluded that particle fraction decrease in the low flow rate branch is mainly because of the distribution in the inlet branch.

2.3 Micro Particle Tracking Velocimetry

2.3.1 μPTV and μPIV

As described in section 1.3, Micro Particle Tracking Velocimetry (μPTV) is used to obtain the velocity vector of the particle by tracking particle, On the contrary, μPIV is used obtain the vectors for a group particles in images by determine the mean of displacement. μPIV is derived from the term of Particle Image Velocimetry (PIV) that first emerged in 1984 and the idea of PIV was came from the method known as Laser Speckle Velocimetry (LSV). The terms of PIV was proposed by R. J. Adrian to distinguish the particles concentration on image plane from speckle mode [1] and allow the individual particles could be observed. To date, PIV has more than 30 years history, it is widely applied in education, fluid dynamics, medical and biology research. Micro Particle Image Velocimetry (μPIV) technique was proposed to investigate the velocity vector of micro-sized particles in a microfluidics device.

The cross-correlation is a measure method for vector in PIV or μPIV analysis. Firstly, the detection of emission light from the traced particles from the different exposures must be recorded on two separate frames. Divide the images into interrogation areas and evaluated [21]. The evaluation of these areas will generate a maximum peak and corresponding velocity and direction. Inversely, the auto-correlation method has only single recorded frame. Compare to cross-correlation, this could only generate the data for velocity and no data for the direction.The image divided into interrogation areas, where the area consists random distribution of particle images.

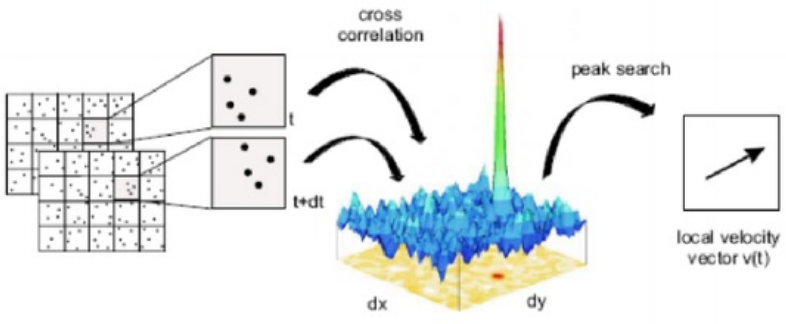

Figure 2.6: Cross-correlation for μPIV. Image from Hemati.

However, to approaching the μPIV techniques, better know the fundamental concept of μPIV is the definition of velocity, u, Eulerian measure method is applied in PIV techniques and yields equation 2.30, where the terms of x and t represents the displacement and time respectively,

$$\vec{u} = \frac{\partial \vec{x}}{\partial t}, \tag{2.30}$$

Relatively, μPTV applying Lagrangian measurement method, this yields the velocity as:

$$\vec{u}(x(t),t) = \frac{\partial \vec{x}}{\partial t}, \tag{2.31}$$

Traceable particles are used for tracking the particle in the fluid, such as fluorescent dyed particles so that particles is visible under the microscope. The images are usually recorded or captured through the PTV or PIV microscopic system or fluorescent microscope which consists a camera with a charge coupled device (CCD) chip. An illuminated light or will transmit through a filter cube with prism, shine on the traceable particle, and the particle will emit the light back to the objective and detector of the camera to record the image.

In addition, the significant difference of the PIV compared to other flow measurement techniques such as Laser Doppler Velocimetry and etc. is that PIV can provide two-dimensional (2D) and three-dimensional (3D) vector fields, while others can only determine the velocity at single point. PIV techniques split the flow images into many small 'interrogation' areas to generate one velocity vector for each areas, this method in PIV has been reckoned to obtain the vector field from the images easily. Each individual particle is identified separately in PTV, and be discovered again in the next frame. The vector in PTV are not placed sometimes and difficult to eliminate its false vector data. However, this give the vector field in PTV enable tracking of particles and can be used calculate again. [38]

Chapter 3

Device Fabrication and Experimental Setup

3.1 Device Fabrication

3.1.1 Photolithography

Photolithography is also known as UV lithography and the photolithography process combines a series of procedures in sequence in microfabrication. Its major process is to "print" a series of patterns from a film onto a substrate by using ultraviolet (UV) light. A photolithography mask is used as template in photolithography process such as fabricate Deterministic Lateral Displacement (DLD) array pattern on a silicon wafer. The photolithography mask is a chrome metal absorbing opaque film with covered material such as glass also known as Soda Lime or fused quartz [8]. On the mask, these covered materials are the transparent areas, they have the high accuracy and tiny etched patterns such as integrated circuit (IC) or DLD array patterns which is created by designer. Therefore, these transparent areas with pattern will allows projected ultraviolet (UV) light to shine through and transfer the patterns onto wafers. The UV light will shine on the exposed SU-8 negative photoresist as stated in Section 3.1.2.

3.1.2 SU-8

SU-8 is a epoxy-based negative photoresist with excellent photosensitivity, good adhesion and high aspect ratio. The name of SU-8 is derived from 8 epoxy groups which consists of Bisphenol A Novolac epoxy, organic solvent and photoacid generator. The SU-8 was formulated and patented by International Business Machines Corporation (IBM) in 1989 [7] [20]. The applications of SU-8 include microelectromechanical systems (MEMS) and microfabrication such as microfluidics channels etc. The resist also gives high chemical resistance, structural stability and low absorption coefficient. In the process of exposure under UV light, a strong acid is formed due to photochemical reaction and initiate cross-linking reaction. However, the cross-linking reaction is not efficient at room temperature

and this can be optimised by thermal treatment process, known as Post Exposure Baking (PEB). The GM1070 data sheet from Gersteltec Sarl. [2] is referred for the microchip device fabrication.

In order to fabricate a Deterministic Lateral Displacement (DLD) array pattern on silicon wafer or fabricate a master wafer, a set of procedures are listed below. To obtain a decent coated wafer and microfludics device, these procedures and following steps in section 3.1.3 and 3.1.4 should be carried out in the clean room to reduce pollutants such as dusts occur on the wafer and microfluidics device.

1. Substrate Preparation

   To obtain the reliability of the following fabrication process, prepare a new and clean substrate such as silicon wafer and oxidate plasma at 200W and 300 mTorr in a plasma cleaner for 5 minutes. After that, pre-bake the wafer on a hot plate at 120°C for 5 minutes. This removes any water from the wafer and improve the adhesion of the photoresists for following steps. Then, cool down the substrate or wafer before spin coating the SU-8 photoresist. Alternatively, solutions that made with acetone or isopropyl alcohol as known as isopropanol can be applied to clean the wafer and also remove any contamination is present on the surface of the wafer.

2. Spin Coating

   Vacuums the silicon wafer on vacuum chuck in the spinner machine and centralise it to ensure the resist will spread evenly upon spinning. Pour a small amount of GM1070 SU-8 photoresist on the wafer. The spin speed on the wafer is dependent of the film thickness in μm, see appendix A.1. During the spin coating process, the extra photoresist might present on the edge of wafer. Thus, removes the edge bead with a surgical blade on the outside edge of spinning wafer at the end of spin. To prevent contamination of the chuck and pins by the photoresist, the acceleration and deceleration ramps should be about 100 rpm/s or the resist will damage the spin coat system. In addition, the ideal time to spread SU-8 photoresist evenly after acceleration ramping in the spin coating process is between 40 seconds to 100 seconds as recommended in figure 3.1.

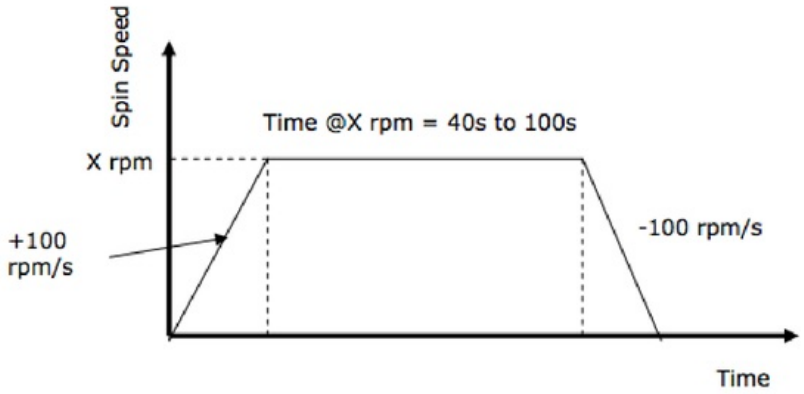

Figure 3.1: Spin speed against time. Image from GM1070 Datasheet.

3. Soft Bake

   Soft bake the wafer with coated SU-8 in two steps. Soft bakes the wafer at 2°C/min ramping from prescribed temperature depending on photoresist thickness and hold for designated time, then continue soft bake with 2°C/min ramping until the temperature reaches between 95°C and 100°C and hold for a longer time, see Appendix A.1. Both of the steps are designed to reduce the "wrinkles" form on the coated wafer for a better photolithography outcome in following step. A hotplate is recommended to use in the soft baking process compare to a convection oven. In addition, hotplate is better than the oven in thermal control and uniformity, yet a skin might present on the coated resist and it can inhibit the evolution of solvent, resulting in incomplete drying of the film and/or extended bake times [33]. After that, leave the wafer on the hotplate to cool down till approximately 45°C.

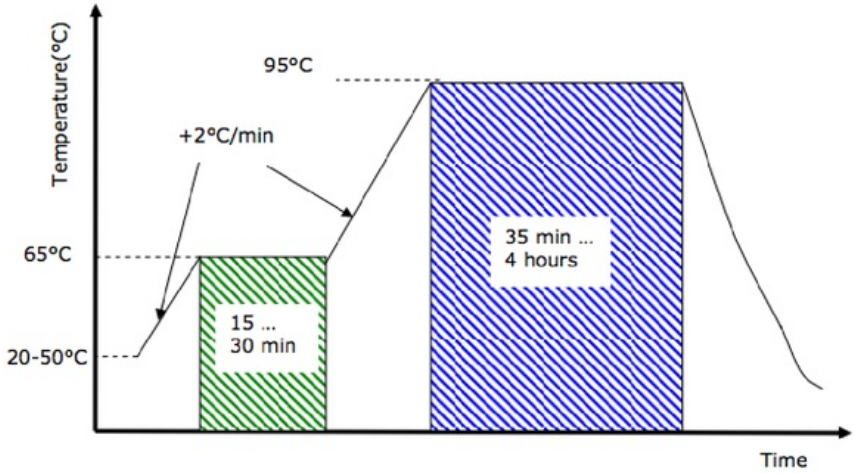

Figure 3.2: Temperature profile against time for soft bake. Image from GM1070 Datasheet.

4. Mask Alignment and Exposure

   Critical steps in the fabrication. This step is to "print" the pattern on the SU-8 coated wafer by exposing UV light through the photomask with a mask aligner. Firstly, align the photolithography mask with the wafer. Expose to the 360 low pressure (LP) UV light at 9mJ/cm^2 in two 10.1 seconds exposures with 15 seconds interval break to limit heating occurs chemical reaction and allows some of the photoresist to be removed in post exposure bake step. Then, delay or rest the wafer at room temperature for 15 to 30 minutes, this is to generate more homogeneity on the amplification phenomenon due to chemical diffusion on exposed areas. The exposure energy is depending on the photoresist thickness and also the UV light parameters of the mask aligner. The exposure dose adjusts the negative wall profile whom slope closed to 90°. To avoid the effects such as cracks, non-sticking or unbalance of size and height of resists patterns while selecting the parameters of dose such as exposure time and adjust focal point of mask aligner. Over-exposure and under exposure will occurs oversizing or incomplete resist patterns.

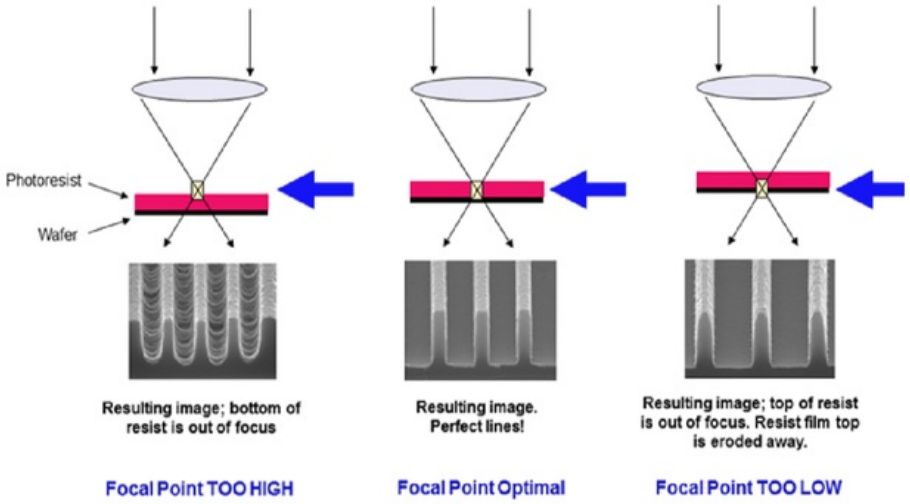

Figure 3.3: Illustration of resulting images due to various focal points. Image from IMM [25].

5. Post Exposure Bake (PEB)

   The following step after exposure and delay is to bake the wafer at similar temperature profile as soft bake with prescribed time, see appendix A.1. The baking process is to help reducing standing wave forms due to exposure under UV light. At the mean time, this also accelerates the cross-linking of the exposed areas making them insoluble in the developer because forming cross linking under room temperature is not efficient after exposure step. Note this step is critical and convection oven is not recommended.

6. Development

   Develop the exposed areas or cross linked areas in propylene glycol methyl ether acetate (PGMEA) or SU-8 developer with constant agitation and used in bath ("old" and "new") for prescribed time to finalise the side wall profile. The recommended development time is dependent on the thickness, see appendix A.1. Then, rinse the wafer with isopropyl alcohol and dry it by using an exhaust with appropriate air pressure of nitrogen.

7. Hard Bake

   Hard bake step or final cure step is optional dependent on the effects on wafer after development steps. If there are some effects occur such as un-sticking SU-8 or cracks after drying, hard bake the wafer to further cross link the SU-8 mould and ensure the mould will be preserve after Polydimethylsiloxane (PDMS) Soft

Lithography steps. Higher temperature profile and similar temperature ramps will be applied in hard bake step compare to the previous baking steps and dependent on the thickness of SU-8.

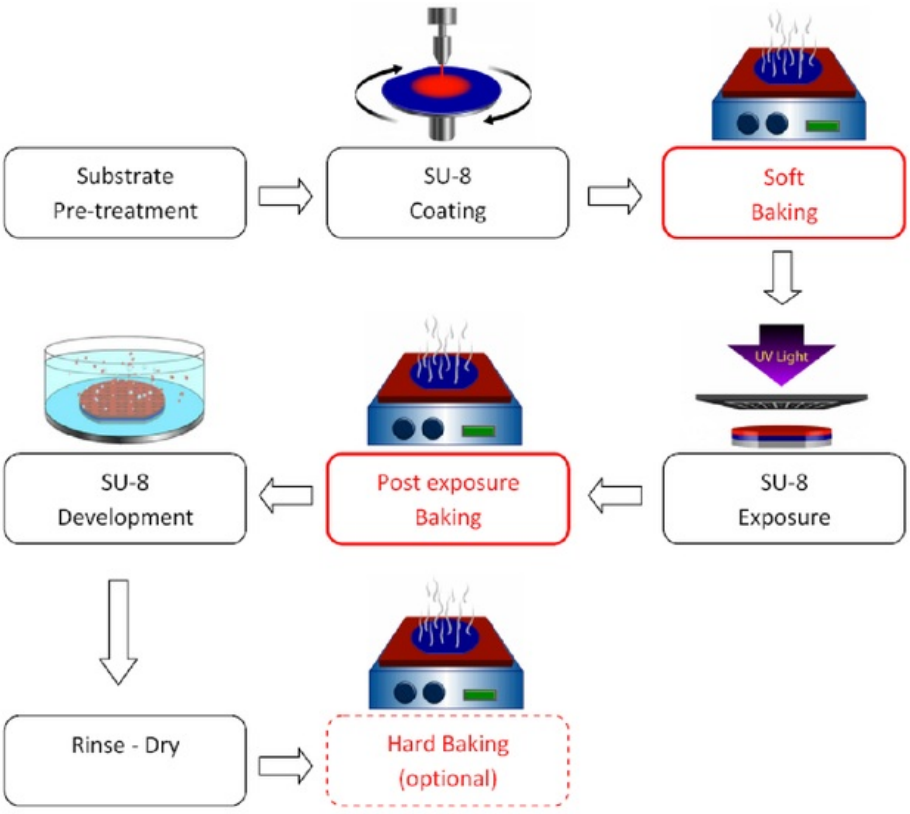

Figure 3.4: Illustration of photolithography process with SU-8. Image from Elveflow [17].

3.1.3 Polydimethylsiloxane (PDMS) Soft Lithography

Soft lithography is a patterning techniques by using polymer as stamp or mould and generate the pattern from master such as SU-8 developed silicon wafer or other master substrates. Multiple soft lithography fabrication methods has been created in the last 20 years including microcontact printing-μCP, replica moulding and microtransfer molding-μTM as presented in figure 3.5 [19].

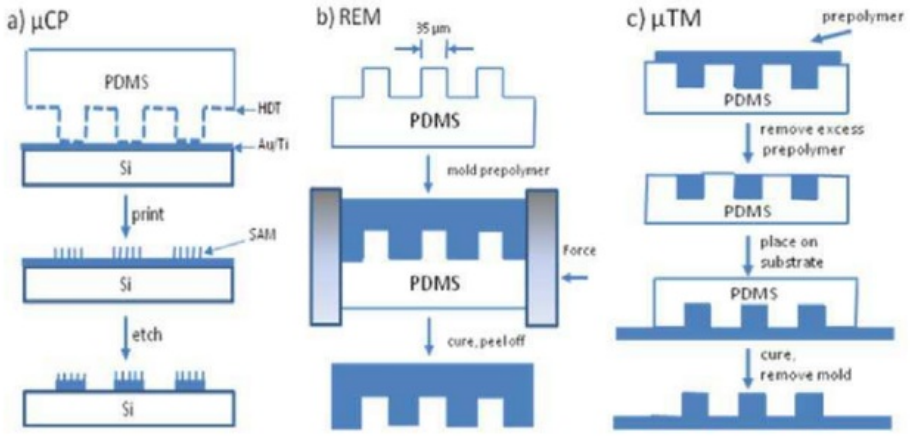

Figure 3.5: Illustration of soft lithography fabrication methods. Image from Flores et al., 2010.

Polydimethylsiloxane (PDMS), known as silicone rubber is widely applied in the fabrication of mircofluidics device due to its lower cost, ease for fabrication, biocompatible and transparency for observing fluorescent molecules. For example, moulding DLD array pattern from a SU-8 coated wafer. In the fabrication, replica moulding technique is applied to fabricate the microchip. Firstly, to create the PDMS pre-polymer, following items are required.

- Sylgard 184 Silicone Elastomer Base
- Sylgard 184 Silicone Curing Agent

Mix an amount of silicone elastomer base and curing agent with the ratio 10:1. Stir the mixture evenly and place the mixture in a vacuum desiccator at -90kPa for at least 15 minutes to degas the mixture. This is preventing bubbles generate and damage the DLD pattern on the wafer or the PDMS. After the mixture fully degassed, pour the PDMS over the DLD pattern on the wafer. Thickness of the PDMS is dependent on the experiment or microchip requirements. Then, bake the wafer with PDMS mixture in the oven at 65°C for at least 2 hours. After baking or PDMS is hardened , peels the PDMS off from the wafer carefully with a tweezer. The DLD array pattern imprinted on the PDMS layer and punch the holes through inlet and outlet positions on the PDMS layer for the following step, Oxygen Plasma Bonding. As an optional before bonding, microscopic on the PDMS with DLD pattern to check the structure whether well forming or not, a cross sectional of PDMS layer can be used to observe and determine the parameters of the pillars.

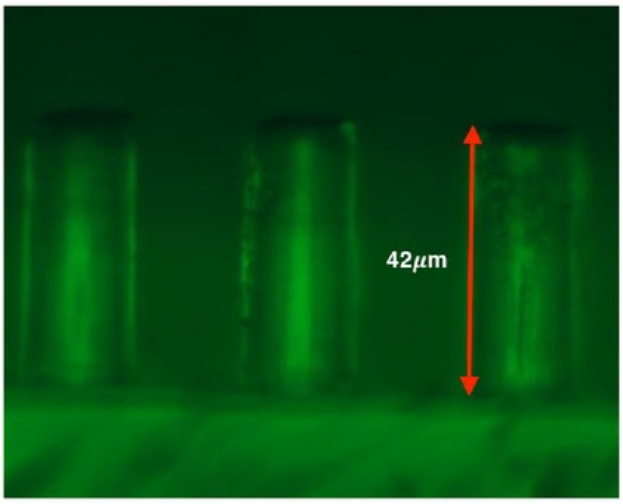

Figure 3.6: Optical microscopy image of a cross-section of PDMS layer

3.1.4 Oxygen Plasma Bonding

Face the PDMS layer with microchannels or DLD array patterns and the cover glass or glass slide for plasma oxidation in a plasma cleaner. The purpose of this process is to change the chemistry on the PDMS surface whilst generate silano terninations (SiOH) on the surface and allow the PDMS bonds with glass slide or cover glass in completely sealed or established condition. To process the plasma oxidation for PDMS layer and glass, set the plasma cleaner to process at 300mTorr and 10W, and plasma on for 22 seconds. Note, ensure the PDMS layer and glass slides are reasonably clean and dry, clean with detergent water and dry with air if it is dirty or fingerprints present. After plasma oxidation, bond the exposed surfaces of PDMS layer and glass slide nicely and give small amount of pressure or press gently to make sure two surfaces are fully bonding with each other and prevent bubbles between the two surfaces. Alternatively, place the microchip in oven for few minutes for harden the PDMS layer bonding with glass.

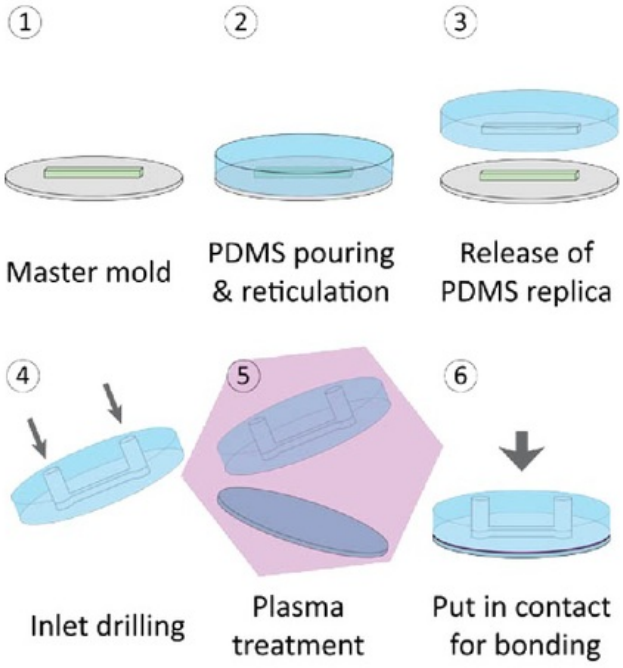

Figure 3.7: Illustration of soft lithography and bonding steps. Image from Eveflow [15].

The fabrication of microchip with DLD array is completed. Submerge the microchip in deionized water, then degas in the vacuum desiccator and prepare for the experiments. Submerge the microchip back into the degassed water if it is not used or after the experiments. This purpose allows to reuse the microchip multiple times, preserve the pattern in PDMS layer of microchip and also prevent contaminants present on microchip.

3.2 Experimental setup

Before the experiment proceedings, set up a number of laboratory equipments and corresponding settings, which are listed and presented in the following figure.

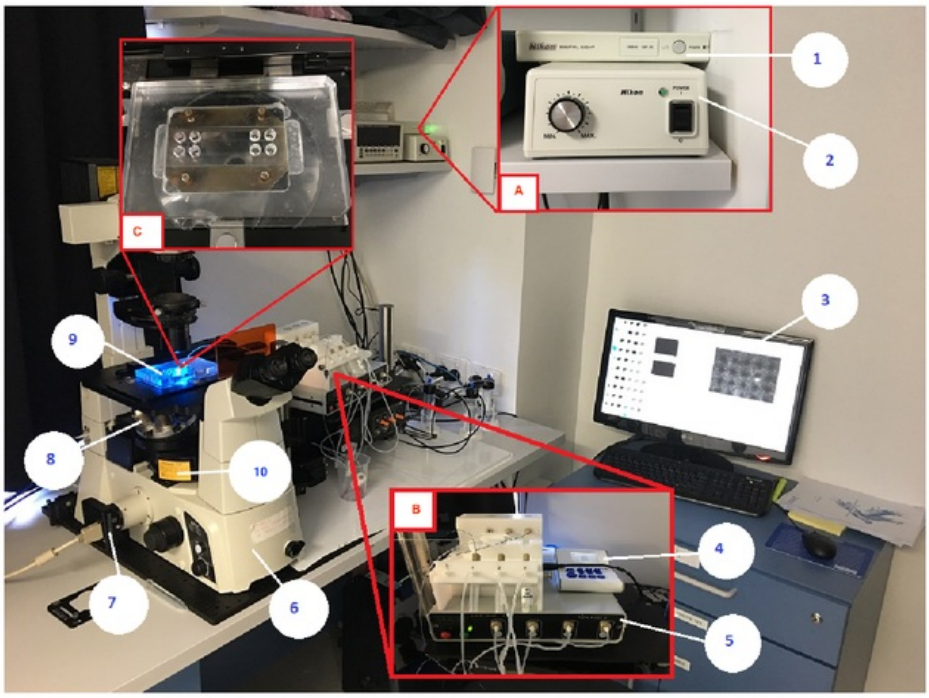

Figure 3.8: Schematic of equipment setup for the experiments

1. Nikon Digital Sight DS-Qi1Mc camera Power Supply, see figure 3.8 (A).
2. Nikon Eclipse Ti-U microscope Power Supply, see figure 3.8 (A).
3. Computer used for manipulate pressure on the pressure controller that connect to microchip and capture images or record videos.
4. CoolLED pE-300 White provide board spectrum LED illumination for imaging fluorescent stains, see figure 3.8 (B).
5. Fluigent MFCS-4C pressure controller, see figure 3.8 (B).
6. Nikon Eclipse Ti-U inverted microscope.
7. CCD digital camera for microscope, Nikon Digital Sight DS-Qi1Mc camera connected with microscope.
8. Microscope objectives or object lenses, Nikon S Fluor 40X/0.90 objective is applied for the experiments.

9. Microchip tighten adequately with chuck, microchip will break if too much force applied due to fragility of the glasses, as shown in figure 3.8 (C).

10. Turret housing for fluorescence filter cubes.

3.2.1 Solution Mixture

In the experiments, a solution mixture containing the fluorescent dyed microspheres, is required for microscopic to obtain the flow field and also the interactions between microspheres with periodic structure in the microfluidics device. The fluorescent dyed microspheres absorb the light and emit back to the fluorescent filters cube. A list of solution mixture recipe is provided as table 3.2. Mix the solutions in a suitable tube and put into ultrasonic bath for at least 3 minutes for mixing throughly. Then, assemble the pipe into the tube that connect with pressure controller for the experiments as shown in figure 3.8 (B).

No.	Solution	Size	Volume
1	Yellow Green Microspheres	0.5μm	20.4μl
2	Suncoast Yellow Microspheres	7.3μm	14.4μl
3	Deionized Water		410.4μl
4	Pluronic F108 with water	200g/l	12μl
5	Glycerol		14.4μ l

Table 3.1: Solution recipe

Descriptions of the solutions:

1. Fluoresbrite[1] 0.5 micron (μm) Yellow Green Microspheres from Polyscience Incorporated is used for the mixture. This yellow green microspheres have fluorescence excitation or absorption maxima at the wavelength of 441nm and emission maxima at 485nm. The Coefficient of Variation (CV) or standard deviation of of the 0.5 micron microspheres is 3% and there is 3.64 x 10^{11} particles per millilitre. They are widely used in mircofludics research, flow cytometry and diagnostic assays. [27]

[1]Fluoresbrite is a registered trademark of Polyscience Incorporated.

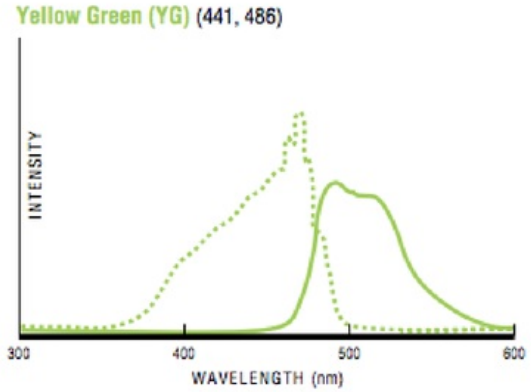

Figure 3.9: Excitation and emission spectra of Yellow Green. Image from Polyscience Incoporated.

2. 7.3 micron (μm) Suncoast Yellow Microspheres from Bangs Laboratories Incorporated is applied for the mixture. The suncoast yellow dyed microspheres have fluorescence excitation maxima and emission maxima at the wavelength of 540nm and 600nm respectively. The CV of the 7.3 micron suncoast yellow microspheres is 0.53 and a number of 4.596 x 10^7 microspheres per millilitre.

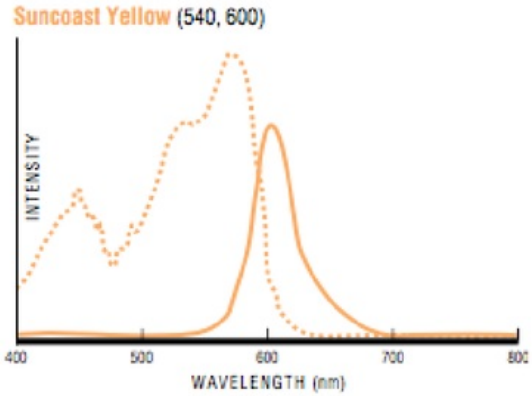

Figure 3.10: Excitation and emission spectra of Suncoast Yellow. Image from Bangs Laboratories [26].

3. Deionized water also known as DI water. The mineral ions, cations such as calcium, iron, sodium and anions such as chlorides and carbonate are removed by ion exchange resins that use hydrogen and hydroxide ions to exchange the mineral ions

and form the DI water [41]. The purpose of the addition of DI water is to dilute the solution mixture. Despite the clean water can be used to dilute the mixture, the mineral ions in the water could damage or block the channel in the microfludics device.

4. Pluronic[2] F108 or known Poly (ethylene glycol)-block-poly (propylene glycol)- block-poly (ethylene glycerol) which is a block copolymer surfactant and nonionic. The viscosity of Pluronic F108 is 2.8 milli Pascal second at 77°C and the average molecular weight is 14600. The surfactant is made in powder or crystals form and it can be dissolved in water. The surfactant is widely applied as cleaners for hard and soft surface, defoamers in coatings and lubricant. In microfludics device, the Pluronic F108 helps to avoid cell or applied particles sticking to the surface and it also gives good stabilization due to its high hydrophilic content [37]. Apply the Pluronic F108 surfactant at ratio 200 grams of surfactant with 1 litre of water and apply 12μl for the solution mixture.

5. Glycerol or glycerin is viscous liquid which is also colourless and odourless. The density of the glycerol is 1.26 grams per millimetre and the viscosity is 1.412 Pascal second. The glycerol is widely apply in molecular biology research such DNA diagnostics and food industry as sweetener due to its sweet tasting and non-toxicity. The glycerol also has good solubility in water and alcohol as well. The reason of applying the glycerol into the solution mixture is to provide stabilization of the mixture for the experiments [36].

3.2.2 Fluorescence Microscopy

Fluorescence is the term that describes the excitation and emission of light by organic and inorganic substances. In 1852, George Gabriel Stokes gave the first description of fluorescence from his observation on light emission of mineral fluorspar which had illuminated by UV excitation and resulting longer wavelength of emitted light than the excitation of light [40]. The applications of fluorescence, including fluorescent light bulb or lamps, stationery such as highlighters, and mineralogy, medicine, scientific research and microscopy as well. The fluorescence microscopy and the experiments should be carried out in dark environment, this will allow better observation on fluorescence dyed microspheres, otherwise will affect the observations and results taken in experiments.

Fluorescent Filter Cube

The fluorescent filter cube plays an important role in the fluorescence microscopy, a filter cube containing the excitation and emission filters and a dichromatic mirror or known as beamsplitter mirror which used to separate and transmit the fluorescence light. The Nikon inverted microscope that used for the experiments has a rotating turret housing for

[2]Pluronic is a registered trademark of BASF Corporation.

selecting appropriate fluorescence filter cube for microscopy. The microscope is connected with the LED illumination system that excites the fluorescent stains to the microscopic object such as fluorescent dyed microspheres. The lamp or LED light is transmitted through the excitation filter and reflected by a dichromatic mirror, pass through the objective lens and towards the fluorescent microspheres in the microchip. Then, the fluorescent dyed microspheres will absorb the filtered light and emit the fluorescence light which is dependent on their dyed fluorescence colours through the mirror and then emission filter. The emission light will be received by the detector on the digital camera or observed through eyepiece. Whilst the activities of microspheres are observed by using the CCD digital camera on the microscope, the activities of the microspheres and the images will be shown synchronistically in the computer monitor by switching the observation output to the digital camera.

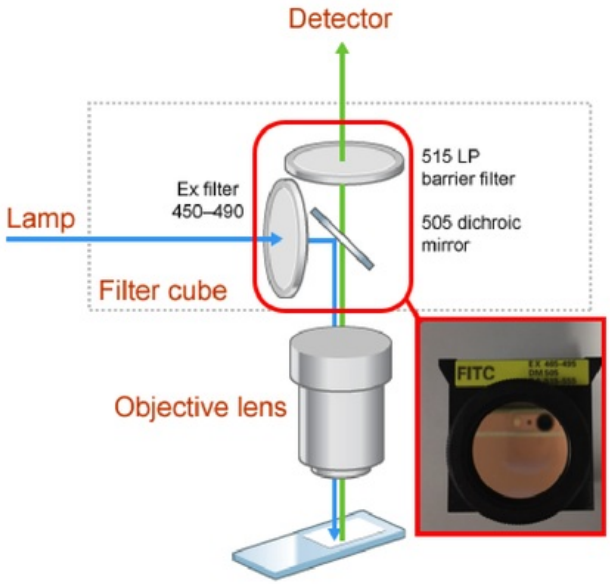

Figure 3.11: Illustration of excitation and emission fluorescence light path. Image from Australian Microscopy & Microanalysis Research Facility [18].

As presented in figure 3.11, the excitation (EX) filter that applied for the experiments has the wavelength ranging within 465 to 495 nanometer and 505 nanometer for the dichromatic or dichroic mirror. Due to emission wavelength of suncoast yellow microspheres that in solution mixture, the 585/40 fluorescence emission filter or barrier filter replaced the filter with the range of wavelength within 515 to 555 nanometer to transmit the emission light effectively from the suncoast yellow microspheres which emission spectra of the microspheres is up to 600 nanometer.

Objective

In the fluorescence microscopy, the objective or objective lens is used to transmit the light to the microscopic object. On the other hand, the objective lens is mainly used to focus on the microscopic object. The focus on the object is dependent on magnification and numerical aperture of the objective lens. The depth of field is determined the distance of the object plane in focus, and it is measured in micrometres for microscopy. A table of depth of field and image depth with various magnifications and numerical apertures as presented in table 3.2. In addition, a Nikon S Fluor 40x objective lens will be used for the following experiments.

Magnification	Numerical Aperture	Depth of Field	Image Depth
4x	0.10	55.5μm	0.13mm
10x	0.25	8.5μm	0.80mm
20x	0.40	5.8μm	3.8mm
40x	0.65	1.0μm	12.8mm
60x	0.85	0.40μm	29.8mm
100x	0.95	0.19μm	80.0mm

Table 3.2: Depth of field and image depth in different magnifications [39].

Chapter 4

Experiments Results and Discussions

4.1 Experiments Results

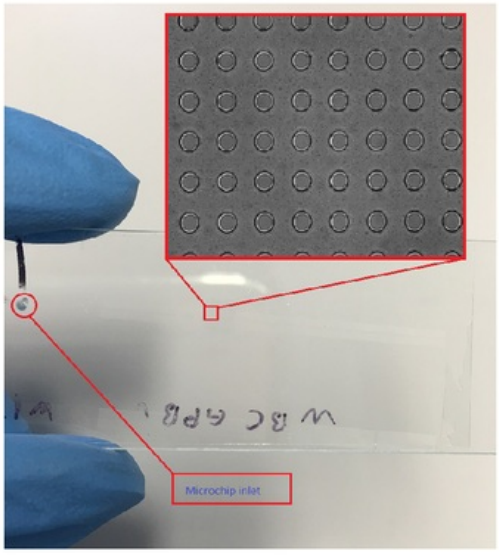

Figure 4.1: Microchip

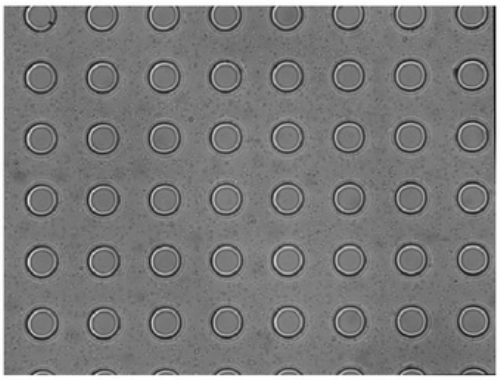

Figure 4.2: Reference image of periodic structure

In following experiments, numbers of videos and images are recorded captured for generate the velocity vector fields. The flows entrained the 0.5 micron and 7.3 micron beads or microspheres as prepared before the experiments, see section 3.2.1. Observed the activities of microspheres at the same location and about middle depth of focus with the 40x objective lens with the gain of 1 or 1.5. The pressure rate of flow controller that applied for the solution mixture enter the microfluidics device at around at around 5 to 25 mBar, pressure rate lower than 5 mBar or equal to 0 mBar will occur reverse flow in the device. In addition, lower the exposure or intensity profile of live videos in digital camera software to give visibility of the smaller beads. The periodic structures in the middle location of device are observed as presented in figure 4.1. The figure 4.2 represents the periodic structure in the microchip.

4.1.1 Running Matlab code

In on order to get the results of the vector plot, Matlab code execution is provided in appendix B or and a step by step description is listed as below:

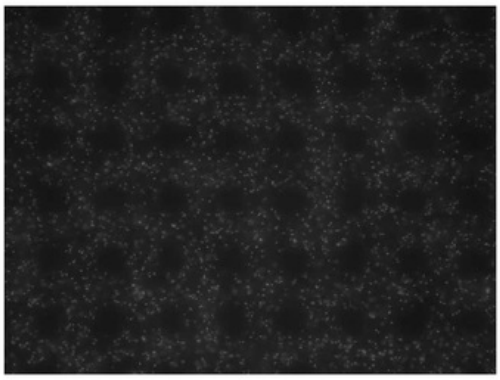

Figure 4.3: Sample image of original video (captured030-gscale.avi).

In figure 4.3, shows the image for the recorded video (captured030-gscale.avi) with no 7.3 micron particle and the recorded video was taken in 640x480 video size with 2x2 binning and the exposure of 40ms and gain of 1 on microscope.

```
clear
filename = 'captured030-gscale.avi'; %insert the recorded video's filename
xyloObj = VideoReader(filename); %read the video
vidWidth = xyloObj.Width; % determines width of movie
vidHeight = xyloObj.Height; % determines height of movie
N=xyloObj.NumberOfFrames; % determines number of frame of movie
```

Create clear function at the beginning of the code. This is to clear the workspace data once the code execute. Set a filename as captured030-gscale.avi and then set another variable, xyloObj to read the video. Determine the width and height of the video and then determine the number of frames in the video. These data will show in the Matlab workspace, N = 399, vidHeight = 480, vidWidth = 640.

```
movRaw = struct('cdata',zeros(vidHeight,vidWidth,3,'uint8'),...
    'colormap',[]); % creates a structure which will hold movie data
peaks = struct('coords',zeros(400,2));
%creates structure to hold bead coordinates
centers = struct('coords',zeros(400,4));
%creates structure to hold refined bead coordinates
graymov=zeros(vidHeight,vidWidth,N,'uint8');
%creates an empty 3D matrix to hold grayscale frames
filtmov=zeros(vidHeight,vidWidth,N,'uint8');
%creates an empty 3D matrix to hold grayscale frames of filtered movie
xyloObj = VideoReader(filename); % reinitialize the video object
```

Creates a structure named movRaw to hold the movie data such as vidWidth, vidHeight. 1x1 struct will be shown in the workspace. Then creates another structure to hold the bead coordinates, and named peaks. Next, creates a structure named centers,

to hold the refined bead coordinates. After that, creates two empty 3D matrix to hold grayscale frames and grayscale frames of filtered movie. The graymov and filtmov will have the value 480x640x399 unit8 in workspace. Call the xyloObj to reintialize the video.

```
k = 1;
positionlist = [0,0,0];
while hasFrame(xyloObj)&& k<100 % check the first 100 frames of video
    movRaw(k).cdata = readFrame(xyloObj);
    % converting video object to structure
    graymov(:,:,k) = imadjust(rgb2gray(movRaw(k).cdata));
    %create grayscale frame in simple 3D matrix
    filtmov(:,:,k)= bpass(double(graymov(:,:,k)),1,5);
    threshold = 0.5*max(max(filtmov(:,:,k)));
    peaks(k).coords = pkfnd(filtmov(:,:,k),threshold,7);
    % record peak coordinates from frame k
    centers(k).coords = cntrd(double(filtmov(:,:,k)),...
        double(peaks(k).coords),9);
    % refines the bead centers to sub-pixel resolution
    A=k*ones(length(centers(k).coords(:,1)),1);
    positionlist = [positionlist; centers(k).coords(:,[1 2]) A];
    k=k+1;
end
    k=k-1;
    link=track(positionlist,9); track
```

Let k = 1, this to create a loop. Then, create a positionlist = [0,0,0] to store the value in the loop. Start the while loop with calling xyloObj's frames and make a condition, k¡100 to allow the loop run 100 hundred times, in here is too run the first hundred frames in xyloObj. Next, in the loop, converting the video object to the structure movRaw. Set graymov(:,:,k) as the action above to create grayscale frame in simple 3D matrix by using rgb2gray function. Then set the filtmov(:,:,k) as above, to smooths the image and deducts the background off, from the graymov array by using bpass[1] and set the wavelength cutoff in the pixels at 1 and 5.

Set the threshold as above and this gives a value at 56 in workspace. Then, records the peak coordinates from frame k by using function pkfnd [2], this will give all the peak location beyond the threshold value. Next, refines the bead centers to sub-pixel resolution, by using cntrd [3] function. Set a variable, A as above and this give the value of 667x1 double in workspace. Next, call the positionlist to record the data then end the loop and call k=k-1. Call the track[4] function to track the data in positionlist, this constructs n-dimensional trajectories of list of particle coordinates and determined at discrete time. The track function give first results of 50% of the data and then 100% of the data that have been tracked. The result show in the command window with 100 of 100 done is tracking 614 particles and 6167 tracks in total.

[1]More details of bpass, available at : http://site.physics.georgetown.edu/matlab/code.html
[2]More details of pkfnd, available at : http://site.physics.georgetown.edu/matlab/code.html
[3]More details of cntrd, available at : http://site.physics.georgetown.edu/matlab/code.html
[4]More details of track, available at : http://site.physics.georgetown.edu/matlab/code.html

```
j=1;
for i=1:(length(link)-1)
    if link(i,4)==link(i+1,4)
        u(j)=link(i+1,1)-link(i,1);
        v(j)=link(i+1,2)-link(i,2);
        x(j)=link(i,1);
        y(j)=link(i,2);
        if u(j) <0
            j=j+1;
        end

    end
end
```

Set j=i, then create a for loop by set i =1 as well. Then this loop is to generate multiple variables that represents the x and y coordinates, and u and v with represents the velocity vector.

```
figure(1)
imshow(filtmov(:,:,k),gray); %show grayscale filtered image
hold on
quiver(x,y,u,v,2); %create the flow field vectors
```

Here, set the command of figure(1) to create a window, then show the grayscale filtered image as presented in figure 4.4. Call hold on function, and plot the quiver with scale size 2, quiver plot will be presented on the grayscale filtered image as shown as figure 4.5.

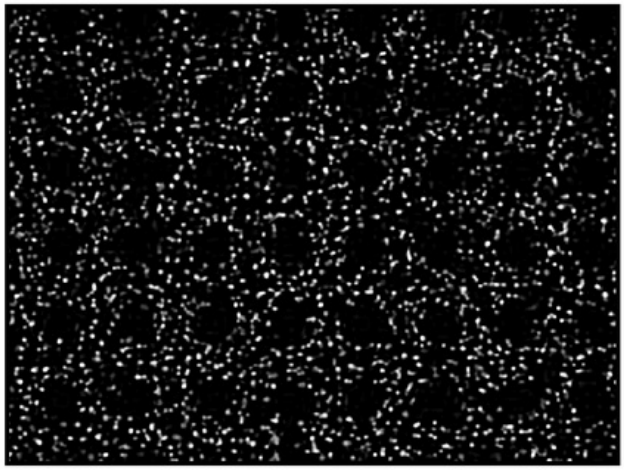

Figure 4.4: Grayscale filtered image

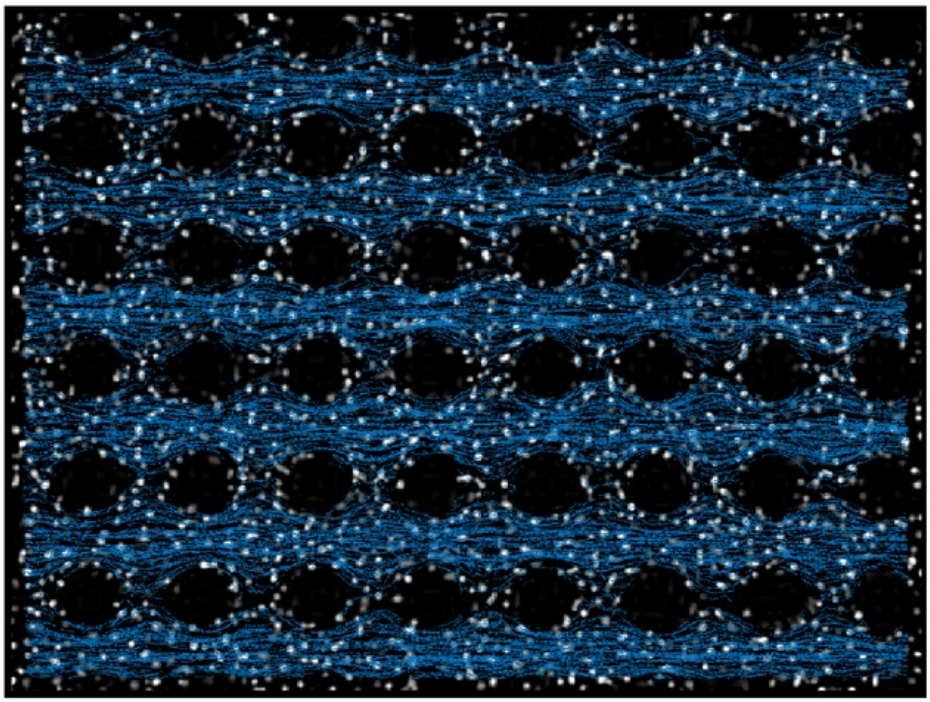

Figure 4.5: Grayscale filtered image

In figure 4.5, shows the vector with scale size of 2, and also shows that less vector occurred in between the pillars.

```
figure(2)
excel =[x',y',u',v']; %transpose the vectors

p=64; % generate the vectors in 64x64 resolution
for i=1:p
    for j=1:p
        % find indices of u and v in the transposed vectors
        % which are within the sector to sector by dividing the movie
        ind=find(excel(:,1)<(vidWidth/p)*i & ...
            excel(:,1)>(vidWidth/p)*(i-1) & ...
            excel(:,2)<(vidHeight/p)*j & ...
            excel(:,2)>(vidHeight/p)*(j-1));

        uavg(i,j)=mean(excel(ind,3)); %average u vectors
        vavg(i,j)=mean(excel(ind,4)); %average v vectors
        xp=(vidWidth/2)/p*(1:1:p);  %x-coordinates
        yp=(vidHeight/2)/p*(1:1:p); %y-coordinates
```

```
        hold on
        q=quiver(xp(i),yp(j),uavg(i,j),vavg(i,j),2);
        % present modified average velocity vectors field
        q.Color='red';
        q.LineWidth=0.5;
        q.MaxHeadSize=1;
    end
end
hold off
```

This part is to generate the vectors in 64x64 resolution, but first we need to transpose the previous data of x, y, u, and v. Then let p = 64 and create a loop. Find the indices which location in the condition. Then, get the mean values for u and v by finding the mean from the transposed array. Then, create the vector plot in default background with arrow scale size of 2. Thus, the code generate a vector plot in 64×64 resolution. The vector plot as presented in figure 4.6.

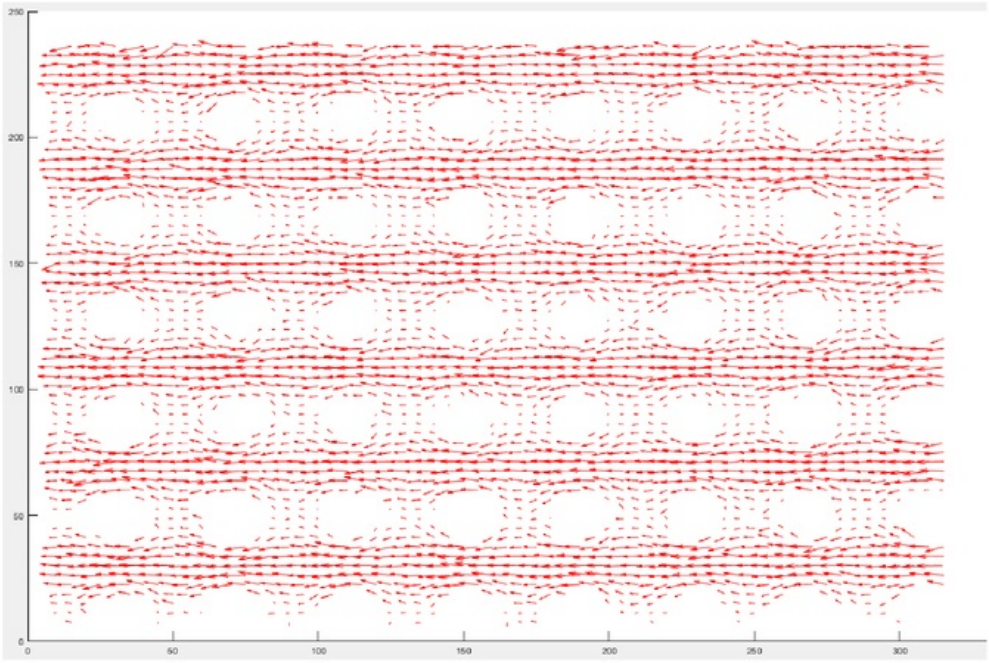

Figure 4.6: Velocity vector field in size of 64×64 with 0.5 micron beads.

In the figure 4.6 shows the average velocity field which simulated the data from previous figure, the vector field looks decent but there are some noise data occurred. The vectors field is plotted in a white background and the vectors formed in curved shape near the pillars along with the flow direction. The velocity vectors u and v are collected for average the rest vector data from other videos at same location.

```
%type in command window
%another option : csvwrite('filename',variable)
xlswrite('082-222uavg',uavg); %xlswrite('filename',variable), then press enter.
xlswrite('082-222vavg',vavg);
```

Then, recorded the variable uavg and vavg for generating the average sum of the velocity vector field. Next, repeat the step and start from clear, for next three video which at the same location.

```
clear

figure(3)
rgb = imread('nobigbeadbackground.tif'); %background image with 640x480
imshow (rgb);

p=64; %generate the vectors in 64x64 resoulution
for i=1:p
    for j=1:p
        xp=(640)/p*(1:1:p);
        %determine the x-coordinates for locating the vector
        yp=(480)/p*(1:1:p);
        %determine the y-coordinates for locating the vector

        %read the collected vectors file
        %for .xlsx file, use xlsxread('filename')
        u1 = csvread('030uavg.csv');
        v1 = csvread('030vavg.csv');

        u2 = csvread('031uavg.csv');
        v2 = csvread('031vavg.csv');

        u3 = csvread('032uavg.csv');
        v3 = csvread('032vavg.csv');

        u4 = csvread('033uavg.csv');
        v4 = csvread('033vavg.csv');

        ut = (u1+u2+u3+u4)/4;
        vt = (v1+v2+v3+v4)/4;

        hold on
        %vector plot with the arrow size of 2.5 and vector properties
        q=quiver(xp(i),yp(j),ut(i,j),vt(i,j),2);
        q.Color='red';
        q.LineWidth=0.5;
        q.MaxHeadSize=2;
    end
end
hold off
```

Here, the code is to generate to the average of sum of velocity vector field, and insert

the background image which is an image from the video.

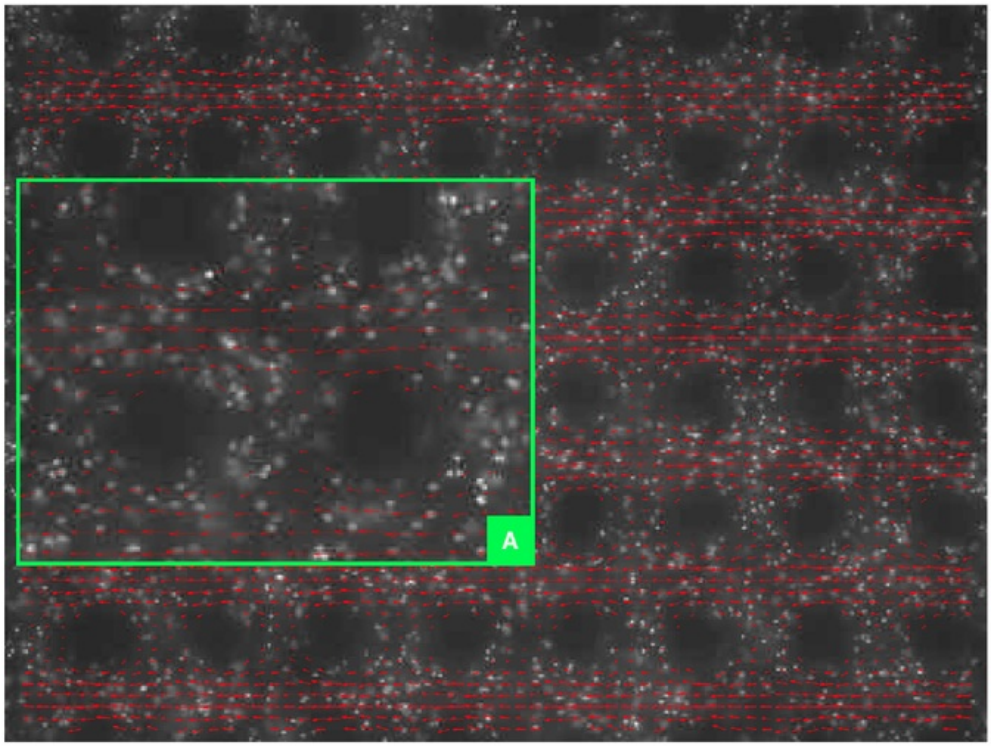

Figure 4.7: Average of sum of velocity vector field in 64×64 resolution with background image

In the figure 4.7 shows the average velocity vectors field from four recorded video data. In the figure, basically this vector flow field is similar to the average vector plot in figure 4.6, but some of the noise data occurred and some vectors unable to quantify between the pillars, see the figure 4.7 (A). On the other hand, the average velocity vector field shows in the figure 4.7, the vectors plot is well formed in curved shape near the pillars along with the flow.

4.1.2 Vector plot results.

Another experiments of the DLD structures with no 7.3 micron particle, but this experiments was recorded with 1.5 gain on the microscopic and the microchip are not similar as the previous. The purpose of using 1.5 gain in the experiment is to try justify the missing velocity vector, by zoom in the image and detect more 0.5 micron beads data. However, the average of total velocity vector field in figure 4.8 shows that there are some

of the vectors between the pillars are not able to quantified in the plot, yet more noise data is generated than the vector field in figure 4.7. Besides, some of the vectors heads (or arrow heads) in the middle stack on the next vectors tails though the scale of vector is decreased to 1.

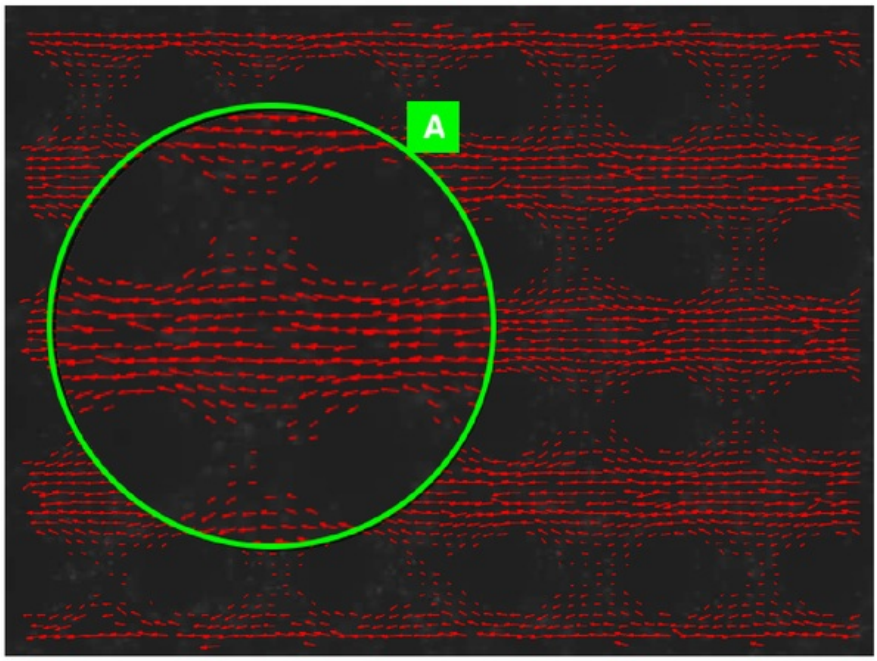

Figure 4.8: Average velocities flow field in 64×64 resolution with 1.5 gain

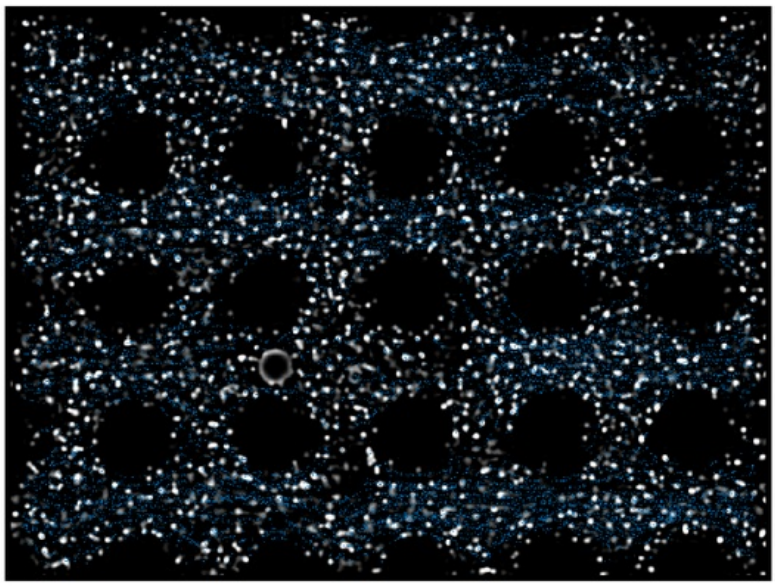

Figure 4.9: Vector field with stationary 7.3 micron particle with arrow scaled size at 0.5.

In figure 4.9 shows the filtered and gray-scaled image with a stationary 7.3 micron particle. As presented in the figure, there are numbers of vectors flow the stationary particle as the flow vector. The following figure 4.10 gives the results of average the sum of the velocity vector, there is no velocity vector go across the stationary bead but the vector field around the stationary bead does not seem ideal. Similarly, the noise data occurred and some of the vector between the pillars could not be quantified. There are some areas in the middle of the flow unable to justify the velocity vector, see figure 4.10 (A).

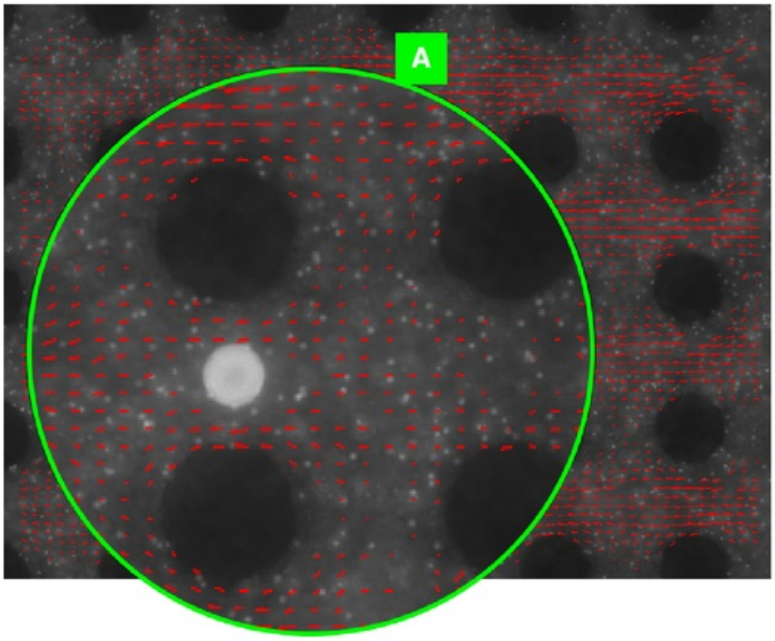

Figure 4.10: Average velocity vector field in size of 64×64 with a stationary 7.3 micron particle.

4.2 Discussions

The possibility that cause some of the vectors cannot be quantified including focus of the objective lens to the array and particles, the small beads between the pillars could be out of the image plane or focus and become lesser readable data or undetectable after bandpass filter function in the simulation code. The present of noise data in the vector plot may caused by higher illumination intensity or exposure time during the experiments and recording the video. However, the noise data can be overcome by optimizing the simulation code with cross-correlation function to eliminate the noise data in interrogation areas with another areas.

To obtain the nice result around the stationary particles, the vector data of images with no big particle can be used to subtracted by the images with stationary big particles, this should give some of the vector that occurred around the stationary particle.

For the moving 7.3 micron beads experiments, the simulation code are not suitable to evaluated a moving bead video directly as other experiments did. However, the noise data is generated and obvious and the figure similar to the figure in experiment with no 7.3 microns particle. This is because of moving particle is followed by the small beads,

once it move to another position in next frame, the initial position will be replaced by small beads. To overcome this problem, is to created a simulation code and detect the array posts location and the main frame where the particle has the bumping mode on it. Find the main frame in the recorded video and crop an area around the location of array post and simulate numbers of the images with the same area size.

Chapter 5

Conclusions and Future Work

5.1 Conclusions

In the thesis, numbers of the microfluidics device with the DLD periodic structures have been fabricated through a series of microfabrication procedures and a numbers of experiments are simulated by Matlab code with the μPTV concept was developed to determine the movement of particles and generate the velocity vector fields. However, from the results and discussion given in the chapter 4, we know that the simulation code does not perform decently in some of the recorded videos. Yet the simulation code has not achieved to perform more details in averaging or eliminate the noise data in the corresponding areas.

According to the objective in early of the project is to provide a good nice velocity vector plot and a series of data regarding the activities of 0.5 micron and 7.3 microns microspheres in a DLD array and evaluated by a μPTV techniques. However, current state of the project can only provide some of the data with 0.5 micron beads and the vector field with a stationary 7.3 micron particle.

5.2 Future Work

The thesis still have much space for development and achieve its final objective. Generate a decent μPTV simulation code to work out on distinguish the noise data and quantify the vectors effectively between the pillars will be the priority for the thesis in the future. However, the properties of the recorded images should be taken into account for getting nice images and that will ease the process on simulate the code. Apply the 100X objective lens to observed the particle clearer and . If the μPTV code successful and this could provide the data of the particle interactions against the DLD array in 2D dimensional or even 3D dimensional and also multiple relevant informations for the future researcher on this field.

Chapter 6

Abbreviations

FSI	Fluid Structure Interactions
DLD	Deterministic Lateral Displacement
μPTV	Micro Particle Tracking Velocimetry
PTV	Particle Tracking Velocimetry
PDMS	Polydimethylsiloxane
μPIV	Micro Particle Image Velocimetry
PIV	Particle Image Velocimetry
LSV	Laser Speckle Velocimetry
MEMS	Microelectromechanical Systems
CCD	Charged Couple Device
IC	Integrated Circuit
UV	Ultraviolet
IBM	International Business Machines Corporation
PEB	Post Exposure Baking
LP	Low Pressure
PGMEA	Propylene Glycol Methyl Ether Acetate
CV	Coefficient of Variation
EX	Excitation

Appendix A

Technical and Product Datasheets

A.1 GM1070 Datasheet

Thickness	15µm	25µm	50µm	100µm	150µm	200µm
Spin coating 40s at ...	5000 rpm	3100 rpm	1700 rpm	900 rpm	650 rpm	400 rpm
Relax. Time*	> 1 hour	> 1 hour	> 1 hour	> 1 hour	> 1 hour	> 1 hour
Pre-bake	15 min @65°C, 35 min @95°C	15 min @65°C, 35 min @95°C	15 min @65°C, 2 hours @95°C	15 min @65°C, 2 hours @95°C	30 min @65°C, 4 hours @95°C	30 min @65°C, 4 hours @95°C
Typical Exposure dose mJ/cm²	475 mJ/cm²	620	800	1000	1200	1300
Post-Bake	15 min @65°C, 40 min @95°C	15 min @65°C, 40 min @95°C	15 min @65°C, 40 min @95°C	15 min @65°C, 40 min @95°C	15 min @65°C, 40 min @95°C	15 min @65°C, 40 min @95°C
Delay time	10 min	10 min	10 min	10 min	10 min	10 min
Develop** in PGMEA	2 min	3 min	4 min	5 min	8 min	22 min
Hard Bake (option)	2h @135°C	2h @135°C	2h @135°C	2h @135°C	2h @135°C	2h @135°C

Figure A.1: Typical processes for different film thickness. Image from GM1070 Datasheet.

Appendix B

Matlab Code

B.1 Vector plot

The Matlab code as shown below, which is used to present the flow field of the beads and generate a size of 64×64 velocity vector field. Instead of plotting the vector field in the end, the code also implies to tracking the particles and their tracks by tracing the high intensity points (or white colour points) frame to frame.The following code is also applied to present the flow fields for the experiments with stationary 7.3 micron beads.

```
% Generate the simple vectors field for recorded video/movie
% Generate velocity vectors field without background image

clear
filename = 'captured030-gscale.avi'; %insert recorded video's filename

xyloObj = VideoReader(filename); %read the video
vidWidth = xyloObj.Width; % determines width of movie
vidHeight = xyloObj.Height; % determines height of movie
N=xyloObj.NumberOfFrames; % determines number of frame of movie

movRaw = struct('cdata',zeros(vidHeight,vidWidth,3,'uint8'),...
    'colormap',[]); % creates a structure which will hold movie data
peaks = struct('coords',zeros(400,2));
%creates structure to hold bead coordinates
centers = struct('coords',zeros(400,4));
%creates structure to hold refined bead coordinates
graymov=zeros(vidHeight,vidWidth,N,'uint8');
%creates an empty 3D matrix to hold grayscale frames
filtmov=zeros(vidHeight,vidWidth,N,'uint8');
%creates an empty 3D matrix to hold grayscale frames of filtered movie
xyloObj = VideoReader(filename); % re initialize the video object
k = 1;
positionlist = [0,0,0];
while hasFrame(xyloObj)&& k<100 % check the first 100 frames of video
    movRaw(k).cdata = readFrame(xyloObj);
```

```
    % converting video object to structure
    graymov(:,:,k) = imadjust(rgb2gray(movRaw(k).cdata));
    %create grayscale frame in simple 3D matrix
    filtmov(:,:,k)= bpass(double(graymov(:,:,k)),1,5);
    threshold = 0.5*max(max(filtmov(:,:,k)));
    peaks(k).coords = pkfnd(filtmov(:,:,k),threshold,7);
    % record peak coordinates from frame k
    centers(k).coords = cntrd(double(filtmov(:,:,k)),...
        double(peaks(k).coords),9);
    % refines the bead centers to sub-pixel resolution
    A=k*ones(length(centers(k).coords(:,1)),1);
    positionlist = [positionlist; centers(k).coords(:,[1 2]) A];
    k=k+1;
end
  k=k-1;

 link=track(positionlist,9);

j=1;
for i=1:(length(link)-1)
    if link(i,4)==link(i+1,4)
        u(j)=link(i+1,1)-link(i,1);
        v(j)=link(i+1,2)-link(i,2);
        x(j)=link(i,1);
        y(j)=link(i,2);
        if u(j) <0
            j=j+1;
        end

    end
end

figure(1)
imshow(filtmov(:,:,k),gray); %show grayscale filtered image
hold on
quiver(x,y,u,v,2); %create the flow field vectors

figure(2)
excel =[x',y',u',v']; %transpose the vectors

p=64; % generate the vectors in size of 64x64
for i=1:p
    for j=1:p
        % find indices of u and v in the transposed vectors
        % which are within the sector to sector by dividing the movie
        ind=find(excel(:,1)<(vidWidth/p)*i & ...
            excel(:,1)>(vidWidth/p)*(i-1) & ...
            excel(:,2)<(vidHeight/p)*j & ...
            excel(:,2)>(vidHeight/p)*(j-1));

        uavg(i,j)=mean(excel(ind,3)); %average u vectors
        vavg(i,j)=mean(excel(ind,4)); %average v vectors
```

```
        xp=(vidWidth/2)/p*(1:1:p);  %x-coordinates
        yp=(vidHeight/2)/p*(1:1:p); %y-coordinates

        hold on
        q=quiver(xp(i),yp(j),uavg(i,j),vavg(i,j),2);
        % present modified average velocity vectors field
        q.Color='red';
        q.LineWidth=0.5;
        q.MaxHeadSize=1;
    end
end
hold off
```

After getting the velocity vector field, record the "uavg" and "vavg" variable in separated file such as Microsoft Excel file (.xlsx) or .csv file by typing the code below into the command window of Matlab. These file will be used to generate the average velocity vector field.

```
%type in command window
%another option : csvwrite('filename',variable)
xlswrite('082-222uavg',uavg); %xlswrite('filename',variable), then press enter.
xlswrite('082-222vavg',vavg);
```

B.2 Average vector plot

Presented Matlab code is used to present the average the recorded vectors and plot the velocity vector field on a background image which is the image from the taken video. Similarly, this code is also used to present the flow fields for the experiments with stationary 7.3 micron beads

```
%Average the velocity vectors that collected from multiple videos...
%at the same location.

%Generate the velocity vector field with background image.
clear

figure(3)
rgb = imread('nobigbeadbackground.tif'); %background image with 640x480
imshow (rgb);

p=64; %generate the vectors in 64x64 resoulution
for i=1:p
    for j=1:p
        xp=(640)/p*(1:1:p);
        %determine the x-coordinates for locating the vector
        yp=(480)/p*(1:1:p);
        %determine the y-coordinates for locating the vector
```

```
        %read the collected vectors file
        %for .xlsx file, use xlsxread('filename')
        u1 = csvread('030uavg.csv');
        v1 = csvread('030vavg.csv');

        u2 = csvread('031uavg.csv');
        v2 = csvread('031vavg.csv');

        u3 = csvread('032uavg.csv');
        v3 = csvread('032vavg.csv');

        u4 = csvread('033uavg.csv');
        v4 = csvread('033vavg.csv');

        ut = (u1+u2+u3+u4)/4;
        vt = (v1+v2+v3+v4)/4;

% Section incomplete, For distinguish noise data
%         s=size(excel(ind,3));
%         if s(:,1)<4
%             uavg(i,j) =0;
%             vavg(i,j) =0;
%         end
%

        hold on
        %vector plot with the arrow size of 2.5 and vector properties
        q=quiver(xp(i),yp(j),ut(i,j),vt(i,j),2);
        q.Color='red';
        q.LineWidth=0.5;
        q.MaxHeadSize=2;
    end
end
hold off
```

Appendix C

Image Processing Toolbox

C.1 ImageJ

ImageJ is a open source program for image processing. ImageJ can generate or process the image or video through a series of function including display, edit, analyze, process, image mathematics, 8-bit colour and grayscale and 32-bit floating point images. ImageJ also supports image stacks, calculate area and pixel value provide corresponding statistics data. In addition, Besides, it can generate histograms and profile plots. It supports standard image processing functions including images, contrast manipulation, sharpening, smoothing, On the other hand, ImageJ also supports third-party plugin or toolbox and also allow to generate custom tools using macros code. [24]. In the project process, ImageJ is used to manipulate the image such as gray scale the video, adjust the brightness, cropping, image calculation etc. The following figures shows the function of Z-project on recorded videos.

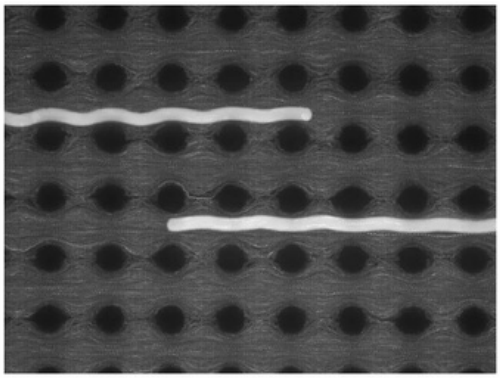

Figure C.1: Processed Image of the video of 7.3 micron moving particles on the gain of 1 on microscope.

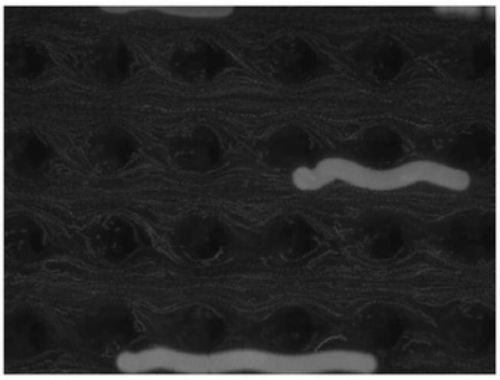

Figure C.2: Processed image of the video of 7.3 micron moving particles on the gain of 1.5

Both of figures (C.1 and C.2) are processed by the function, Z-project, to present the motions of the 7.3 microns particle and 0.5 microns particle of each frame and stack together become an image as presented. Apparently, the images were taken on different gain value on microscope and also on two different chip. The figure C.1 shows the upper particle flows along with streamline and bumping, Despite the lower particle is near to pillars, the particle still flow steadily along with the middle streamlines. On the other hand, the particles as presented in figure C.2 are bumping pillars to pillars along with flow.

Bibliography

[1] R. J. Adrian, "Twenty years of particle image velocimetry," *12th International Symposium on Applications of Laser Techniques to Fluid Mechanics*, July 2004.

[2] L. Akesso, *GM 1070 Datasheet*, Jan 2005.

[3] J. Beech, *Microfluidics Separation and Analysis of Biological Particles.* Fasta Tillståndets Fysik, October 2011.

[4] F. Breussin, "Pharmaceutical & biomedical research likely to use $1 billion worth of microfluidics devices by 2016," *Drug Discovery World*, 2012.

[5] J. P. Brody, P. Yager, R. E. Goldstein, and R. H. Austin, "Biotechnology at low reynolds numbers," *Biophysical Journal*, vol. 71, December 1996.

[6] J. Castillo-León and W. E. Svendsen, *Lab-on-a-chip Devices and Micro-Total Analysis Systems.* Springer International, 2015.

[7] F. Chollet, "Su-8: Thick photo-resist for mems," *MEMS Cyclopedia*, December 2013, accessed: 25/10/2016. [Online]. Available: http://memscyclopedia.org/su8.html

[8] Compugraphics. So what is a photomask. Accessed: 1/10/2016. [Online]. Available: http://www.compugraphics-photomasks.com/us/education-centre/what-is-a-photomask/so-what-is-photomask/

[9] C. M. Cyclopedia. Navier-stokes equations. Accessed: 27/8/2016. [Online]. Available: https://www.comsol.com/multiphysics/navier-stokes-equations

[10] J. A. Davis, "Microfluidic separation of blood components through deterministic lateral displacement," *Doctor of Philosophy*, September 2008.

[11] V. Doyeux, T. Podgorski, S. Peponas, M. Ismail, and G. Couper, "Spheres in the vicinity of a bifurcation: Elucidating the zweifach-fung effect," *Journal of Fluid Mechanics*, March 2011.

[12] T. Dracos, *Particle Tracking Velocimetry (PTV).* Springer, 1996, vol. 4.

[13] M. V. Dyke, *Creeping flow.* The Parabolic Press, 1982.

[14] Elveflow. Mircofluidics: A general overview of microfluidics. Accessed: 29/8/2016. [Online]. Available: http://www.elveflow.com/microfluidictutorials/microfluidicreviewsandtutorials/microfluidics/

[15] ——, "Pdms: A review," accessed: 5/10/2016. [Online]. Available: http://www.elveflow.com/microfluidic-tutorials/microfluidic-reviews-and-tutorials/the-poly-di-methyl-siloxane-pdms-and-microfluidics/

[16] ——. Plug and play microfluidic setup. Accessed: 6/11/2016. [Online]. Available: http://www.elveflow.com/microfluidic-flow-control-archive/plug-and-play-microfluidic-setup/

[17] ——. Soft lithography: Su-8 baking. Accessed: 5/10/2016. [Online]. Available: http://www.elveflow.com/microfluidic-tutorials/soft-lithography-reviews-and-tutorials/how-to-get-the-best-process/soft-lithography-su-8-baking/

[18] A. M. . M. R. Facility. Fluorescence microscopy. Accessed: 3/11/2016. [Online]. Available: http://www.ammrf.org.au/myscope/confocal/confocal/fluorescence/index.php?popup=true&iframe=true&width=800&height=600

[19] A. Flores and M. R. Wang, *Soft Lithographic Fabrication of Micro Optic and Guided Wave Devices*, M. R. Wang, Ed. InTech, February 2010.

[20] J. Gelorme, R. Cox, and S. Gutierrez, US Patent US 4 882 245, November 21, 1989.

[21] M. Hemati, "Mirco-particle image velocimetry," *MAE199*, 2007.

[22] S. Holm, J. Beech, M. Barrett, and J. Tegenfeldt, "Separation of parasites from human blood using deterministic lateral displacement," *Lab on a Chip*, February 2011.

[23] L. Huang, E. Cox, R. Austin, and J. Sturm, "Continuous particle separation through deterministic lateral displacement," *Science*, vol. 304, May 2004.

[24] ImageJ. Imagej features. Accessed: 6/11/2016. [Online]. Available: https://imagej.nih.gov/ij/index.html

[25] IMM. Lithography process overview. Accessed: 13/10/2016. [Online]. Available: http://www.imicromaterials.com/technical/lithography-process-overview

[26] B. L. Incorporated. Dye colors & spectra. Accessed: 3/11/2016. [Online]. Available: http://www.bangslabs.com/support/technical-support/spectra-information

[27] P. Incorporated. Fluoresbrite yg microspheres 0.5μm. Accessed: 3/11/2016. [Online]. Available: http://www.polysciences.com/default/fluoresbrite-yg-microspheres-050m

[28] D. W. Inglis, "Efficient microfluidic particle separation arrays," *Applied Physics Letters*, vol. 94, 2009.

[29] D. W. Inglis, J. A. Davies, R. H. Austin, and J. C. Sturm, "Critical particle size for fractionation by deterministic lateral displacement," *Lab on a Chip*, March 2006.

[30] J. C. Jo. (2010, September) Fluid-structure interactions. Accessed: 1/9/2016. [Online]. Available: http://www.eolss.net/sample-chapters/c05/e6-165-01-00.pdf

[31] R. C. Johnson, "Ibm lab on chip detects cancer," *EE Times*, October 2016. [Online]. Available: http://www.eetimes.com/document.asp?doc_id=1330279

[32] J. McGrath, M. Jimenez, and H. Bridle, "Deterministic lateral displacement for particle separation: A review," *Lab on a Chip*, September 2014.

[33] Microchem. Su-8 2000 permanent epoxy negative photoresist processing guidelines for su-8 2100 and su-8 2150. Accessed: 1/10/2016. [Online]. Available: http://www.microchem.com/pdf/SU-82000DataSheet2100and2150Ver5.pdf

[34] O. Reynolds, *An experimental investigation of the circumstances which determine whether the motion of water shall be direct or sinuous, and of the law of resistance in parallel channels.* Royal Society, 1883, vol. 174.

[35] A. Robinson. (2009, November) 2010 ferrari 458 italia - quick spin. Accessed: 28/9/2016. [Online]. Available: http://www.caranddriver.com/reviews/2010-ferrari-458-italia-quick-spin

[36] Sigma-Aldrich. Glycerol. Accessed: 2/11/2016. [Online]. Available: http://www.sigmaaldrich.com/catalog/product/sigma/g5516?lang=en&region=AU

[37] ——. Poly(ethylene glycol)-block-poly(propylene glycol)-block-poly(ethylene glycol). Accessed: 2/11/2016. [Online]. Available: http://www.sigmaaldrich.com/catalog/product/aldrich/542342?lang=en&region=AU&gclid=CK3kjpahitACFQqkvQodCoELxA

[38] B. Sokoray-Varga and J. Józsa, "Particle tracking velocimetry (ptv) and its application to analyse free surface flows in laboratory scale models," *Periodica Poltechnica*, October 2008.

[39] K. R. Spring and M. W. Davidson. Depth of field and depth of focus. Accessed: 3/11/2016. [Online]. Available: https://www.microscopyu.com/microscopy-basics/depth-of-field-and-depth-of-focus

[40] ——. Introduction to fluorescence microscopy. Accessed: 3/11/2016. [Online]. Available: https://www.microscopyu.com/techniques/fluorescence/introduction-to-fluorescence-microscopy

[41] P. I. Water. What is deionized water. Accessed: 2/11/2016. [Online]. Available: http://puretecwater.com/deionized-water/what-is-deionized-water

[42] Wikipedia. Turbulence. Accessed: 6/11/2016. [Online]. Available: https://en.wikipedia.org/wiki/Turbulence